9-6-2017

Multi-Level Dynamical Parameter Estimation: Hypothesis Testing with Dynamical Systems

Henry S. Harrison
University of Connecticut, henry.schafer.harrison@gmail.com

Multi-level Dynamical Parameter Estimation: Hypothesis Testing with Dynamical Systems

Henry S. Harrison, Ph.D.

University of Connecticut, 2017

ABSTRACT

The practice of dynamical modeling of perception-action behavior has lagged behind the proliferation of the dynamical perspective. Two methodological roadblocks to dynamical modeling are discussed. First, parameter selection is difficult with current tools. Second, it is unclear what role models have in the larger scientific project beyond their use as descriptions or proofs of concept. In this dissertation, a new parameter selection method is developed to address these issues, Multi-Level Dynamical Parameter Estimation (MLDPE). Like its precursor DPE, MLDPE uses an extended Luenberger observer to stabilize the synchronization manifold in combined model-data space. MLDPE also embeds a regression model into the parameter-selection process, allowing for parameter values to vary systematically as a function of both fixed and random effects. In this way, it allows for parameter dynamics to be used as dependent variables in experimental research. The method is tested with three experiments. In Experiment 1, a model of steering dynamics was fit to data while allowing preferred walking speed to vary by participant. In this case, the limitations of local search were encountered due to non-smooth functions in the model equations. Experiments 2 and 3 demonstrated the use of fixed effects in MLDPE, using data collected in a driving simulator with a braking task. Experiment 2 showed that changing the context of the task

from a race to a safety test produced predictable changes in parameter values. Experiment 3 tested the effects of distraction on braking, replicating previous results and describing them in terms of parameter dynamics. Thus, MLDPE is able to select parameters using multiple observations of a system, unlike previous methods. Additionally, it is able to detect changes in dynamics across these observations. This method allows dynamical models to be used in a traditional experimental research program. Possible applications and limitations of the method are discussed.

Multi-level Dynamical Parameter Estimation: Hypothesis Testing with Dynamical Systems

Henry S. Harrison

Sc.B., Brown University, 2009

A Dissertation

Submitted in Partial Fulfillment of the

Requirements for the Degree of

Doctor of Philosophy

at the

University of Connecticut

2017

APPROVAL PAGE

Doctor of Philosophy Dissertation

Multi-level Dynamical Parameter Estimation: Hypothesis Testing with Dynamical Systems

Presented by

Henry S. Harrison, Sc.B.

Major Advisor _____
Till D. Frank

Associate Advisor _____
Tehran J. Davis

Associate Advisor _____
Adam Sheya

University of Connecticut

2017

ACKNOWLEDGMENTS

Many people must be thanked for making it possible to reach this moment. First of all, thanks to Claudia Carello and Michael Turvey for creating this community and welcoming me and so many other interesting people into it; and for making sure that we are always making discoveries but providing beer rations regardless. Thanks to my advisor Till Frank, whose attention to detail always kept me honest; and to Tehran Davis, Adam Sheya, Claire Michaels, J Dixon, Bruce Kay, and Bill Mace, for showing me how much there is to learn, encouraging me to pursue my own research interests, and always keeping me humble. I also owe a special thanks to Bill Warrren for showing me a new way of thinking about behavior and setting me on the path that led to CESPA.

Thanks to all the CESPA friends I've made over the years: Lin Nie, Maurici López, Jason Gordon, Katie Santomoasso, T.R. and Ari Brooks, Vitor Profeta, Gabi Pinto, Adrian Frazier, Dobri Dotov, Stephanie Petrusz, for being reliable sources for a scientific discussion, a laugh, or a gripe, as needed.

Thanks to my parents Brenda Schafer and Jeremy Harrison for all their love and nurturing and for giving me everything I needed to make it here in the first place; and to my siblings Sam, Alex, Charlie, and Emma for always offering an interlude from grad student life when I needed it. Thanks also to the Shield family for their unwavering support and guidance. I owe so much to the strong family environemnt in which I grew up, and now I am blessed to be a part of two amazing families.

Most of all, thank you to my wife Lily Shield, for joining me in this journey; you are my foundation.

Contents

Chapter 1

Introduction

Behavioral dynamics

Gibson (1979/1986) argued that behavioral control does not require a central controller, that behavior can be "regular without being regulated" (p. 225). Gibson's intuitions on perception (and action; Gibson, 1958) were similar to those developed through the study of movement dynamics (Haken, Kelso, & Bunz, 1985; Kelso, 1995; Kugler & Turvey, 1987). These researchers developed the idea that movement patterns could arise from natural laws of nonlinear dynamics and pattern formation. Their work also promoted dynamics as a common language for describing the coupling between the physical world and agents that acted within it. In particular, the discovery that the same dynamical patterns observed in the movements of a participant's fingers (coupled neurally and mechanically through the body) also occurred in the movements of the limbs two participants coupled only visually (Schmidt, Carello, & Turvey, 1990) cemented the idea that coupling is fundamentally a function of information (Kelso, 1995).

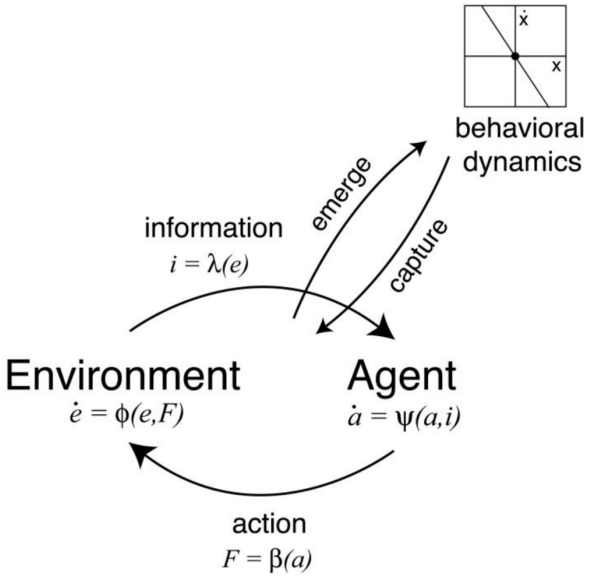

FIGURE 1.1: Warren's (2006) schema of the dynamics of perception of action (p. 376).

Also consistent with Gibson's (1958, 1979/1986) perspective was the view that perceptual information could directly guide goal-direction action (Lee, 1976; Turvey & Carello, 1986; Warren, 1988). Demonstrating the existence of perceptual variables that provided task-specific information strengthened the case for Gibsonian direct perception (Michaels & Carello, 1981). Warren's (2006) *behavioral dynamics* framework formalized this notion. According to behavioral dynamics, just as the physical world is governed by laws of nature, the agent is governed by laws of control, which describe how the agent's movements are modulated by informational variables. Thus, the agent and environment are coupled dynamical systems. From their interaction emerges behavioral dynamics, a low-dimensional description of the agent-environment system. A schema of this approach is shown in Figure 1.1. From this perspective, stable patterns of behavior are not predetermined but rather self-organize as a product of natural law and system dynamics.

Behavioral dynamics is naturally suited to the development of dynamical models; exam-

ples of such models include steering (Fajen & Warren, 2003, 2004; Warren & Fajen, 2004, 2008), braking (Harrison, Turvey, & Frank, 2016; Lee, 1976), following (Dachner & Warren, 2014), and fly-ball catching (Chapman, 1968; Fink, Foo, & Warren, 2009; McLeod, Reed, & Dienes, 2006; Michaels & Oudejans, 1992; Michaels & Zaal, 2002). These models also served to promote van Gelder's (1998) dynamical hypothesis—specifically the knowledge hypothesis: the claim that cognitive scientists should use dynamical models and the concepts of dynamical systems theory in order to best understand behavioral systems. Following Warren (2006), ecological psychology appears to have embraced the dynamical hypothesis. Dynamical systems theory concepts such as *attractor* and *bifurcation* are ubiquitous, but they are typically used as metaphors rather than shown to exist in a (mathematical) dynamical system. Figure 1.1 appears often in conference talks, but is rarely accompanied with more specific equations. My conclusion is that the knowledge hypothesis (van Gelder, 1998) has been embraced conceptually, but the model-building has not seen the same resurgence.

The relative lack of model-building is not necessarily a problem. The concepts of dynamical systems theory are powerful and even without an accompanying model they provide useful intuitions. The value of dynamical systems theory lies in its ability to spatialize systems, allowing one's geometric intuitions to be applied to complex problems. Even when a model is available, its qualitative behavior (its topology) is more important than its precise quantitative predictions. Van Gelder (1998) remarks that the resources of dynamical thinking "can be brought to bear even in the absence of an actual equation-governed model," providing "a qualitative or preliminary understanding of the phenomenon, which may be the best available" (p. 621). Furthermore, the construction of a model is not always feasible; for example, Thelen and Smith's (1994) influential, dynamical perspective on development was developed largely in the absence of explicit models. The motivation for this project, rooted in increasing the accessibility of dynamical modeling, should not be taken as denying

that the importance of dynamics in Psychology lies at least equally in dynamical *thinking* as it does in dynamical modeling.

It should also be noted that the knowledge hypothesis has taken off in a direction not anticipated by van Gelder (1998): the application of dynamics to behavior not with model-building but with complex-systems timeseries analysis methods. This is exemplified by the annual Cognition Dynamics Workshop held at the University of Connecticut, which typically features few dynamical models but a plethora of complex-systems analyses that incorporate dynamical systems theory implicitly, if not explicitly. For example, analyses such as recurrence quantification analysis (e.g., Balasubramaniam, Riley, & Turvey, 2000; Riley, Balasubramaniam, & Turvey, 1999) rely on Takens's (1981) theorem, a mainstay of dynamical systems theory. Additionally, researching incorporating fractality or multifractality (e.g., Dixon, Holden, Mirman, & Stephen, 2012; Harrison, Kelty-Stephen, Vaz, & Michaels, 2014; Kelty-Stephen, Palatinus, Saltzman, & Dixon, 2013; Stephen & Dixon, 2011) does not involve the building of dynamical models, but relies on a dynamical perspective.

Finally, notice should be taken that dynamical models are not exactly rare (e.g., Frank, Profeta, & Harrison, 2015; Harrison et al., 2016; Lopresti-Goodman, Turvey, & Frank, 2013; Richardson et al., 2015). I merely observe that there are not as many as one might expect given the ubiquity of dynamical metaphors in the ecological psychology discourse. Also, although many of the models cited above do indeed describe the dynamics of behavior, they mostly do not utilize Warren's (2006) behavioral dynamics framework in a strict sense.

Considering why behavioral dynamics models are not more widespread, I have reached two hypotheses. First, there are practical reasons why model-building is difficult. Constructing a dynamical model is only feasible for relatively simple behaviors, compared to the phenomena that can be examined using more open-ended dynamical analyses such as multifractality. Furthermore, after building a model, in order to validate it with observed

data, one must fit its parameters. This is a difficult task that often requires more expertise in numerical methods and scientific computing than is required to build the model in the first place. Despite its difficulty, parameter selection is usually uninteresting from a theoretical perspective. Below, I examine the problem of parameter selection in detail.

A second possible explanation for the lack of models concerns their role in a larger scientific project. Van Gelder (1998) anticipates and dismisses the argument that dynamics provide only descriptions and not explanations. I of course agree with this assessment; however, it hints at a more subtle problem: the utility of models. Of course, models have applications, such as driving large-scale simulations (e.g., Klügl & Rindsfüser, 2007; Yersin, Maïm, Pettré, & Thalmann, 2009). But for a scientist interested in explanations, what role do models play? For Warren (2006), specific models play a role akin to a proof of concept. For example, if a dynamical model constructed according to ecological theory—based on the interaction between agent and environment—produces realistic behavior, this demonstrates the *possibility* that ecological theory explains behavior. Once such a possibility is demonstrated, models can provide further explanations, such as identifying perceptual information used to guide action (e.g., Warren, Kay, Zosh, Duchon, & Sahuc, 2001). However, despite van Gelder (1998), the payoff for modeling seems to be greatest when the model's function as a description of the system of interest can serve as proof of concept for the skeptical. For an audience that does not need to be convinced of the plausibility of the underlying concepts, despite their explanatory power, dynamical models have little further utility. Models serve as important proofs of concept, demonstrating that behavior can emerge from interactions between agent and environment. Once that role is fulfilled, however, models are of limited used beyond their capacity to simulate realistic behavior.

In this dissertation, I explore solutions to the first problem, parameter selection in particular. In so doing, I aim to make progress at the second problem, finding a role for dynamical

models to play in ongoing research programs that focus on traditional behavioral experiments rather than dynamical modeling.

Dynamical systems

A vector function $\mathbf{F}$ describes a dynamical system such that

$$\dot{\mathbf{y}} = \mathbf{F}(\mathbf{y}, \mathbf{r}), \tag{1.1}$$

where $\mathbf{y}$ is the (vector-valued) state of the system, and $\mathbf{r}$ is a vector of parameters. Here, dot notation is used to denote the derivative with respect to time. Colloquially, a dynamical system describes the rate of change of the system's state, as a function of the state. Equation 1.1 is thus a system of first-order ordinary differential equations (ODEs). Although dynamical models are sometimes written as one or more second- or third-order differential equations, these must be rewritten in the form of Equation 1.1 before the numerical and analytical methods discussed here can be applied.

Steering dynamics model

Warren (2006) highlights the behavioral dynamics of locomotion as a representative case study for the approach. These dynamics have been elucidated in a series of papers (Fajen & Warren, 2003, 2004, 2007; Warren & Fajen, 2004, 2008) that develop the steering dynamics model and validate it using empirical data. The model serves as a "proof of concept" of behavioral dynamics, demonstrating how stable patterns of behavior (in this case, routes through a cluttered environment) can emerge from purely local, online interactions. Thus, in contrast with path-generation models (e.g., Khatib, 1986), action need not

be planned in advance. Similarly, observed phenomena such as personal space (Gérin-Lajoie, Richards, Fung, & McFadyen, 2008; Gérin-Lajoie, Richards, & McFadyen, 2005), aperture traversal (e.g., Cinelli, Patla, & Allard, 2008; Hackney, Vallis, & Cinelli, 2013), and crowd behavior (e.g., Batty, DeSyllas, & Duxbury, 2003; Helbing & Molnar, 1995) need not be first-class components of a locomotor model but rather may emerge from simple model components (Bonneaud, Rio, Chevaillier, & Warren, 2012). This emergentist account of steering is therefore compatible with the principles of ecological psychology, self-organization, and coordination dynamics (Gibson, 1979/1986; Kelso, 1995; Kugler & Turvey, 1987).

The steering dynamics model simplifies the dynamics of locomotion by isolating the problem of steering. It considers an agent moving at a constant speed through an environment, modeling only the agent's changes in heading as it turns left or right to circumvent obstacles and steer toward a goal. The relevant variables are shown in Figure 1.2. Heading (ϕ) is defined as the agent's direction of travel with respect to an arbitrary reference axis, and bearing (ψ) as the direction of a target or obstacle with respect to the same axis at distance d. The difference between these two angles is the target- or obstacle-heading angle ($\beta = \psi - \phi$).

The steering dynamics model can be broken down into a set of components for stationary and moving obstacles and targets. These components are linearly combined to produce the total influence of the environment on agent's heading. Fajen and Warren (2003) introduced the first two components for stationary targets and obstacles. They formalized the attraction of the agent's heading toward the direction of the goal as an angular damped spring, with spring stiffness (k) determining angular acceleration and damping (b) reflecting resistance to turning. Thus, agents turn toward the goal by nulling the goal-heading angle β_{g} according to the second-order differential equation

$$\ddot{\phi} = -b_{\mathrm{g}}(-\dot{\phi}) - k_{\mathrm{g}}\beta_{\mathrm{g}}(e^{-c_1 d_{\mathrm{g}}} + c_2). \tag{1.2}$$

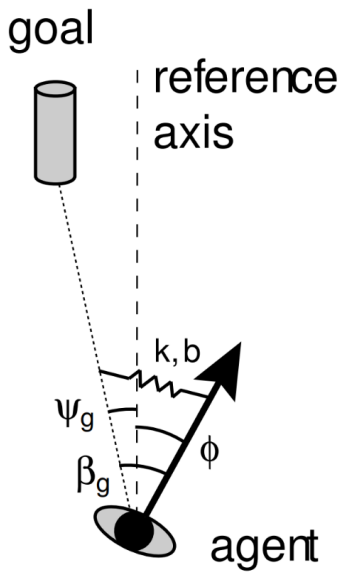

FIGURE 1.2: Definition of variables in the steering dynamics model, from Warren and Fajen (2008): heading direction ϕ, goal direction ψ_g, target-heading angle β_g, stiffness k, and damping b.

The damping term $-b_g$ resists turning and prevent oscillation in heading; the stiffness term $k_g\beta_g$ reflects the control law, providing an attractor in the direction of the goal at $\beta_g = 0$; and the distance modifier $(e^{-c_1 d_g} + c_2)$ dulls the goal attraction as distance to the goal increases. Thus, the parameter c_1 determines how quickly attraction decreases with distance, and c_2 sets a minimum proportion of attraction that remains even at long distances. This model was fit to human data and its parameters determined (using brute force) as $b_g = 3.25$ s^{-1}, $k_g = 7.5$ s^{-2}, $c_1 = 0.4$ m^{-1}, and $c_2 = 0.4$.

The obstacle term (Fajen & Warren, 2003) is effectively the inverse of the goal term, creating a repeller in the direction of the obstacle (obstacle-heading angle $\beta_o = 0$). Thus, the stiffness term is positive rather than negative. Adding a stationary obstacle term to Equation 1.2 results in the following equation:

$$\ddot{\phi} = \cdots + k_o\beta_o e^{-c_3|\beta_o|}e^{-c_4 d_o}. \tag{1.3}$$

The first modifier on the stiffness term reduces repulsion as obstacle-heading angle increases, with the parameter c_3 determining the magnitude of this reduction; the second modifier on the stiffness term modulates heading with distance, with the parameter c_4 serving a similar role as c_1. However, with no parameter analogous to c_2, obstacle repulsion completely disappears at long distances.

Fajen and Warren (2007) concluded that humans intercept moving targets using a constant-bearing strategy, that is, nulling the goal bearing-angle $\dot{\psi}$. Thus, a steering model using this strategy can be expressed as

$$\ddot{\phi} = -b_{\mathrm{mg}}\dot{\phi} - k_{\mathrm{mg}}\dot{\psi}_{\mathrm{g}}(d_{\mathrm{g}} + 1). \tag{1.4}$$

Here, b_{mg} and k_{mg} are moving-goal versions of the damping and stiffness parameters, respectively. The distance modifier $(d_{\mathrm{g}} + 1)$ increases the attraction as distance increases; this ensures that the agent will turn fast enough at long distances. This model was validated by comparing it to three other possible control strategies; the constant-bearing strategy produced the best fit to observed data as well as robustness in the face of perceptual noise.

The final basic component of the steering dynamics model is avoidance of moving obstacles. This model was presented in conference posters (e.g., Cohen, Bruggeman, & Warren, 2005, 2006). Due to difficulties I will discuss momentarily, the manuscript validating the full model with respect to human data remains unpublished (Bruggeman, Cohen, Harrison, & Warren, 2013). An inverse strategy to the moving-goal component was formalized as follows, with the obstacle component added on to either Equation 1.2 or Equation 1.4 (depending on whether the target is stationary or moving):

$$\ddot{\phi} = \cdots + k_{\mathrm{mo}}(-\dot{\psi}_{\mathrm{o}})e^{-c_5|\dot{\psi}_{\mathrm{o}}|}e^{-c_6 d_{\mathrm{o}}}\left(1 - \frac{\left(\mathrm{sgn}\left(\beta_{\mathrm{o}} - \frac{\pi}{2}\right) + 1\right)}{2}\right). \tag{1.5}$$

Here, the stiffness term is modulated such that repulsion decreases with increasing absolute values of $\dot{\psi}$; the parameter c_5 determines the slope of this modulation. Repulsion also decreases with distances according to the parameter c_6 in a similar manner as with the stationary obstacle term. Finally, the complicated-looking modifier including a sign function simply sets repulsion to 0 when the obstacle is behind the agent; otherwise, this takes a value of 1. Thus, agent's trajectories are not affected by moving obstacles that are not in the agent's field of view.

With the moving obstacle component, the issue of walking speed came to the foreground; an assumption of constant speed was no longer viable. This makes intuitive sense when one considers route selection with respect to a moving obstacle (whether one passes the obstacle's trajectory in front of or behind the obstacle). As a result, the constant-speed assumption was abandoned and the dynamics of speed control were examined. The control laws instantiated by Equations 1.2 to 1.5 each revolve around a specific agent-environment relationship that becomes either an attractor (for the goal components) or a repeller (for the obstacle components). These agent-environment relationships can be controlled by changes in heading (as in the above equation) or by modulating speed. In other words, there is not a one-to-one relationship between agent degrees of freedom and perceptual invariants. Therefore, it was argued that speed control may act as an additional degree of freedom recruited in service of a common goal: avoiding constant-bearing angle (in the case of moving-obstacle avoidance). A similar argument for a unified account of the visual control of goal-directed locomotion, involving both speed and heading was given by Chardenon and Warren (2004). Bruggeman et al. (2013) used similar logic to arrive at the following ODE describing

speed changes during moving-obstacle avoidance:

$$\dot{v} = b_v(v - v_\mathrm{p}) + k_v\dot{\psi}_\mathrm{o}(\operatorname{sgn}\dot{\psi})e^{-c_7|\dot{\psi}_\mathrm{o}|}e^{-c_8 d_\mathrm{o}}\left(1 - \frac{\operatorname{sgn}\left(|\beta_\mathrm{o}| - \frac{\pi}{2}\right) + 1}{2}\right). \tag{1.6}$$

The structure of this equation is similar to Equation 1.5, with new parameters. The sign-function modifier is necessary to match acceleration and deceleration with trajectories passing ahead and behind the obstacle, respectively, rather than with leftward or rightward changes in heading. Additionally, the equivalent of the damping term is not centered around zero but around some preferred velocity v_p. As a result, agents are predicted to locomote at $v = v_\mathrm{p}$ until they accelerate or decelerate to avoid a collision.

As a result of adding changes in speed to the model, the number of parameters increased from 7 to 12. Although it might be plausible to set $c_5 = c_7$ and $c_6 = c_8$, the damping and stiffness parameters have different units (because the left-hand-side of the ODE has different units) and therefore cannot be equivalent. Furthermore, it is natural to assume that v_p will not be constant across participants, but rather that each participant will have their own preferred walking speed. In fact, the variation in participant walking speeds is what initially prompted the development of Equation 1.6. Replacing v_p with $v_{\mathrm{p},1}, \ldots, v_{\mathrm{p},N}$, where N is the number of participants, results in $11 + N$ parameters. This made the parameter-selection methods previously used intractable (even with seven parameters, the brute force method is questionable at best) and effectively stalled the project. These difficulties are discussed in more detail under the heading Global optimization. One objective of this dissertation is to solve the parameter-selection problem for the combined heading-speed steering dynamics model.

Affordance-based control model of braking

The second model used in this dissertation was the affordance-based control model of visually guided braking (Harrison et al., 2016). This model extends David Lee's $\dot{\tau}$ strategy (Lee, 1976), according to which drivers brake in order to create and maintain the optical invariant $\dot{\tau} = -0.5$, were τ is the optically specified time-to-contact with the obstacle. By using this strategy, drivers achieve a constant deceleration, coming to a stop as the obstacle is approached.

Fajen (2007) used the $\dot{\tau}$ strategy as a foil with which to critique the use of the information-based control laws associated closely with behavioral dynamics. Calling his approach *affordance-based control* in contrast with the *information-based control* of the models heretofore discussed, Fajen argued that agents move so as avoid crossing action boundaries, beyond which the action goal is no longer afforded. In other words, agents must stay in safe zones, but within those zones, they are free to deviate from control laws.

Harrison et al. (2016) reconciled information- and affordance-based control, formalizing the concept of action boundaries in the language of behavioral dynamics. In their approach, control laws are still used, but their strength (or stiffness) is modulated according to the agent's proximity in state space to the action boundary. Then, the control law could be combined with *soft constraints* that determine the agent's trajectory through the safe zone. Far from the action boundary, soft constraints dominate the control law; close to the action boundary, stiffness increases and the control law dominates, preventing the action boundary from being crossed.

Although Harrison et al. (2016) present several models, here I will consider the ODE

$$\dot{a} = -b(v - v_{\mathrm{p}}) - k\left(\frac{a - a_{\mathrm{ideal}}}{a_{\mathrm{ideal}} - a_{\mathrm{min}}}\right), \tag{1.7}$$

where a is acceleration (the second derivative of position, hence Equation 1.7 is a third-order ODE); v is velocity (another state variable, and the first derivative of position); a_{ideal} is the ideal acceleration (i.e., the deceleration that would produce $\dot{\tau} = -0.5$) itself a function of the state variables; the parameter v_{p} is preferred velocity (its term is a soft constraint); b is a damping parameter, the strength of this preference; k is a stiffness parameter, the base strength of the braking control law; and a_{min} is the minimum acceleration (maximum deceleration), defining the relevant action boundary.

According to Harrison et al.'s (2016) perspective on affordance-based control, soft constraints provide a route for context to influence the manner (see also Shaw & Kinsella-Shaw, 1988) in which a control law is realized. Thus, an objective of this dissertation is not only to fit the parameters in Equation 1.7, but also to determine whether the parameters of the soft-constraint term may vary with experimental context in a predictable fashion.

Parameter selection

Given the definition of dynamical systems in Equation 1.1, parameters are values that remain constant, invariant to time as well as to the system's state. Parameter values are typically not seen theoretically interesting, as they merely tune the model after its structure is already determined (for an exception, see Saltzman & Munhall, 1992, ; I will consider their perspective under the heading Parameter dynamics). Nevertheless, values must be set before the model can be simulated and therefore before its consistency to observed data can be assessed quantitatively. Therefore, selection between competing models requires parameters to be fit for each model before a best-performing model can be selected.

In general, parameter-selection problems take the following form:

> Find values of parameters $\mathbf{r}$ such that the correspondence between simulated trajectories (solutions of Equation 1.1) and observe trajectories is maximized.

Here, I specifically use a vague formulation, as the method used to quantify this notion of "correspondence" is an outstanding problem, or at least a choice that the researcher must make in the parameter-fitting process.

Optimization

In order to solve a parameter-fitting problem, it must be transformed into a more generic optimization problem. Optimization problems take the following form:

$$\begin{aligned} \underset{\mathbf{x}}{\text{minimize}} \quad & C(\mathbf{x}) \\ \text{subject to} \quad & g_i(\mathbf{x}) = 0, \\ & h_j(\mathbf{x}) \geq 0, \end{aligned} \tag{1.8}$$

where $C(\mathbf{x})$ is the cost function; $g_i(\mathbf{x}), i = 1, \ldots, M$ defines M equality constraints; and $h_j(\mathbf{x}) \geq 0, j = 1, \ldots, N$ defines N inequality constraints. Many algorithms exist to solve problems of this class, varying as to which types of constraints they support, whether the objective and constraint functions are always linear or sometimes nonlinear, whether the elements of $\mathbf{x}$ are integers or real numbers, the scale of the problems they work best with, and whether they are able to find global optima or merely local optima. Here, we concern ourselves only with nonlinear optimization in which the values of $\mathbf{x}$ are real numbers.

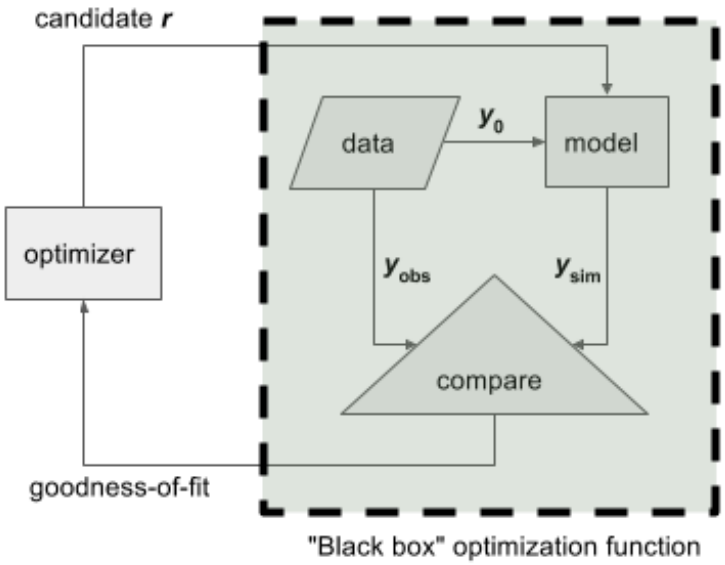

FIGURE 1.3: The naive "black box" approach to parameter selection, in which a parameter set $\mathbf{r}$ is evaluated according to a goodness-of-fit comparison of the resulting simulated trajectory $\mathbf{y}_{\text{sim}}$ to the observed trajectory $\mathbf{y}_{\text{obs}}$.

"Black box" parameter fitting

A naive approach is to identify the optimization values $\mathbf{x}$ with the parameter vector $\mathbf{r}$, and consider only constraints that define valid bounds for the parameter values (e.g., they must be non-negative). Then, the objective function simulates the system, compares simulated trajectories with observed trajectories, and outputs an error measure. This is the method used by Fajen and Warren (2003, 2007), who averaged the trajectories of each experimental condition, and used R^2 between observed (average) and simulated trajectories as their error measure.

This is an example of what we might call a "black box" approach to parameter selection, because the objective function cannot be written out analytically; rather, it is more of a computational routine. Specifically, the reliance on simulation, or numerical solutions, of the system of ODEs renders the objective function inscrutable to the objective function. A

schematic of this approach is shown in Figure 1.3. Here, a number of researcher decisions are elided by the step labeled "compare". Not only must a comparison statistic be chosen (e.g., R^2, squared error, etc.), but in order to evaluate this statistic, simulated states $\mathbf{y}_{\text{sim}}(t)$ must be matched with observed states $\mathbf{y}_{\text{obs}}(t)$. If the observed and simulated trajectories are not of equal duration, they must be somehow cropped or stretched in order to line up their values (note that this same problem must be solved when averaging trajectories). This is by no means an insoluble problem, but there is no solution for the general case, and therefore the researcher must use domain knowledge to arrive at an appropriate method for the specific case. This not only represents extra work for the researcher, but may bring additional assumptions into play that may not hold for all simulated trajectories.

This problem of $\mathbf{y}_{\text{obs}}(t)$ and $\mathbf{y}_{\text{sim}}(t)$ having different durations is only one example of a mismatch that can occur between observed and simulated trajectories when testing a parameter set that is far from the "correct" parameter values. The parameter-selection process attempted for the combined speed-heading steering dynamics model (Bruggeman et al., 2013) provides another example. We were interested in maximizing the consistency between model and data in two respects: the shape of the locomotor path, and also the qualitative route selection—that is, whether the participant avoided the obstacle by walking ahead or behind its trajectory. As a result, an error measure had to be devised that traded off these concerns, reflecting the fact that improving the path shape of a non-matching route may not push the fitting process in the desired direction. Thus, a black-box approach relying on numerical simulations for each candidate parameter set often requires a custom error measure that is specific not only to the dynamical model under study but also the set of conditions used to collect the observations being used for parameter selection.

More generally, simulated trajectories may deviate greatly from observed trajectories, not only in duration but also in state space. As a result, the value of the goodness-of-fit measure

may be somewhat meaningless. It is one thing to compare two similar trajectories; it is another to compare two trajectories with very little resemblance. In this case, relying on a series of small improvements in goodness-of-fit—as most optimization algorithms do—has no guarantee of moving in the direction of the best-fitting parameter values. In more technical terms, the synchronization manifold in combined model-data space may not be stable, and as a result the optimization surface of parameter space will be irregular (see Abarbanel, Creveling, Farsian, & Kostuk, 2009; Quinn, Bryant, Creveling, Klein, & Abarbanel, 2009, for precise definition and mathematical treatment of this instability).

Outside the perception-action literature, this irregularity of parameter-space surfaces is a well-known problem (Pires, Vautard, & Talagrand, 1996; Voss, Timmer, & Kurths, 2004), but within the behavioral-dynamics literature is has not been addressed. As a result, the optimization landscape is likely littered with local optima in which the optimizer is likely to get stuck, unable to find the true global optimum. In addition, other assumptions made in the comparison process may not hold. For example, a natural solution to the problem of different durations is to assume that the trajectories traverse the same space (e.g., between a starting position and a goal), and use the spatial relationship between the trajectories to determine which values to compare (e.g., the methods described in Roduit, 2009). For a poor set of parameter values, however, the simulation may not properly traverse the space at all, and the comparison will fail.

In summary, the black-box approach has the following drawbacks:

- it may be computationally expensive, due the numerical simulations,
- it is analytically inscrutable,
- it requires a custom error measure, reflecting the researcher's priorities,

- it requires comparing timeseries of different durations, and
- it is likely to produce an optimization landscape that is not smooth.

Global optimization

As a result of these drawbacks, researchers are forced to choose from optimization algorithms that are global and gradient-free. Global optimization algorithms are those that are able to solve the problem of local optima. Gradient-free algorithms do not rely on the slope of the optimization landscape (more precisely, the gradient of $f(\mathbf{x})$ with respect to $\mathbf{x}$). Global optimization algorithms such as genetic algorithms and simulated annealing are slow, require many settings to be chosen, and as a result of their heuristic nature are unreliable. There is no guarantee, as there is for local optimization, than the optimum is found. Therefore, the researcher must spend a great deal of time running fits, testing the optimization with different settings, never having much certainty that the best set of parameters has been found. In addition, these settings, along with the choices made during the comparison step, contribute to the degrees of freedom problem, allowing researchers to keep trying new analyses until the desired outcome is attained (Simmons, Nelson, & Simonsohn, 2011).

Early behavioral dynamics research (e.g., Fajen & Warren, 2003) avoided many of these problems for a simple reason: The most naive of all optimization methods, brute force, is a global method. In brute force optimization, every possible combination of parameter values is tested, and the set with the best resulting fit is chosen. Although this avoids many of the problems noted previously, it is only practical for problems with a very small number of parameters, and a very small number of simulations to run for each comparison. For more complicated models, or if the researchers wish to avoid averaging trajectories or allow for the possibility of a parameter varying over participants or conditions, brute force

must be abandoned. Thus, as behavioral dynamics projects proceeded, they eventually ran into the problems described in this chapter. This is what happened to the steering dynamics model, as described previously. Several components of the model were published in succession (Fajen & Warren, 2003, 2007), but in order to describe the avoidance of moving obstacles, model complexity was increased and averaging had to avoided due to variation in participant walking speed. As a result, brute force was abandoned and all the difficulties described in this section were discovered. Despite working on the problem for years, and running global optimization algorithms for months at a time, the parameter-fitting problem was never satisfactorily solved, and the model remains unpublished (Bruggeman et al., 2013).

The status quo, then, is that in order for parameter fitting to keep up with advances in model building (e.g., Harrison et al., 2016), behavioral dynamics researchers must become experts in global optimization. Even so, they are still unlikely to find success. This clearly represents a barrier to entry into behavioral dynamics that must be remedied if behavioral dynamics is to remain as central to ecological psychology as has been claimed (e.g., Fajen, Riley, & Turvey, 2009).

Dynamical Parameter Estimation

Instead of entering the rabbit hole of global optimization, it would be preferable to explore other ways to transform parameter-fitting problems into optimization problems. An ideal solution would be generic; that is, it must be solved only once and the behavioral dynamicist need only to apply the method rather than adjust it for the particular case at hand. Considering all the difficulties discussed in this section, we seek a parameter fitting method that

- is analytically tractable, avoiding numerical simulation in the objective function, so

that the gradient of the objective function can be determined analytically,

- results in a smooth optimization landscape, so that global optimization is not needed,
- does not require an error measure specific to the model and data-collection conditions,
- does not have settings that the researcher must experiment with, and in general does not introduce any new choices, and
- can be run in a reasonable amount of time without requiring a cluster or other advanced processing capabilities.

Most of these requirements are fulfilled by the method of Dynamical Parameter Estimation (DPE), proposed by Abarbanel et al. (2009). DPE provides an alternative to the black-box method for transforming parameter-dynamics problems into optimization problems. The motivation for DPE is to stabilize the synchronization manifold, allowing for smooth surfaces in parameter space.

Before developing these ideas, we must first translate Equation 1.1 into a difference equation of the form

$$\mathbf{y}(n+1) = \mathbf{f}(\mathbf{y}(n), \mathbf{r}), \tag{1.9}$$

with $n \in \{1, \ldots, N\}$ referring to the time step. The conversion from ODE (Equation 1.1) to difference equation (Equation 1.9) can be done using a number of approximate methods, such as Euler or Runge-Kutta.

A common approach for eliminating parameter-space irregularities is to couple observed data to the model by adding a control term (Quinn et al., 2009). For simplicity, consider that only the first dimension of the system is observed, with observed values $x_1(n)$. Then,

the control term is added by replacing the first dimension of Equation 1.9 with

$$y_1(n+1) = f_1(\mathbf{y}(n), \mathbf{r}) + k(x_1(n) - y_1(n)), \tag{1.10}$$

where $k > 0$ is a coupling constant, that, if large enough, forces x_1 to align with y_1. This method is known as a Luenberger observer after the work of Luenberger (1964, 1966, 1971).

As nonlinear systems are typically not homogeneous in state space, it is necessary to include time-dependence in the coupling (Abarbanel et al., 2009) such that

$$y_1(n+1) = f_1(\mathbf{y}(n), \mathbf{r}) + u(n)(x_1(n) - y_1(n)), \tag{1.11}$$

where k has been replaced by a timeseries of coupling strengths $u(n)$. This is known in the control literature as an extended Luenberger observer (Luenberger, 1964, 1966, 1971).

As a result of this synchronization, with the right values of $u(n)$, the model's trajectory will never stray from the data's, regardless of the validity of the parameter set $\mathbf{r}$ or even the validity of the model. Therefore, many of the problems discussed above disappear. There is no longer an issue of model trajectories deviating wildly from observed trajectories, causing irregularities. The fitting process becomes one of minimizing the necessary synchronization.

Abarbanel et al. (2009) propose DPE as a combination of an extended Luenberger observer with the cost function

$$C(\mathbf{y}, \mathbf{r}, u) = \frac{1}{2N} \sum_{n=0}^{N-1} \left[(x_1(n) - y_1(n))^2 + u(n)^2 \right]. \tag{1.12}$$

Optimization can then proceed as a minimization problem of Equation 1.12 over $(\mathbf{y}, \mathbf{r}, u)$.

Note that the synchronization values u are treated on the same footing as the parameters $\mathbf{r}$. Even more divergent from the black-box approach, the optimization vector also

includes the state values $\mathbf{y}$. Instead of including numerical simulations in the procedure, Equation 1.9 (with Equation 1.11 substituted for y_1) are introduced as equality constraints. Therefore, when fitting parameters with DPE, *the model is never simulated*.

In the traditional black-box approach, the optimization vector has length R, where R is the number of parameters $\mathbf{R}$. DPE greatly expands the optimization space, from R to $R + N(D + 1)$, where D is the number of dimensions in $\mathbf{y}$. ND dimensions in optimization space come from $\mathbf{y}$, and an additional N come from $u(n)$. However, this massive increase in the size of the optimization space comes with an additional ND equality constraints, one dimension of a difference equation at each time step. Thus, the only degrees of freedom added to the problem that are not accounted for by constraints are those associated with the synchronization values $u(n)$.

By ensuring that model trajectories stay close to the observations, DPE creates smooth surfaces in parameter space, allowing local optimizers to be used. Furthermore, the cost function, Equation 1.12, is straightforward to differentiate analytically, allowing solvers to take advantage of the objective-function gradients. The equality constraints can also be differentiated analytically with the aid of a symbolic computing engine, allowing the optimizer to use the Jacobian of the constraints. In theory, these advances should greatly improve the parameter-selection experience. A software package that strings together all these steps without user input, and launches a proper optimizer automatically, would allow researchers to fit parameters without becoming experts in numerical optimization.

Model consistency

Abarbanel et al. (2009) propose a method for measure the overall consistency between model and data, at the conclusion of the parameter-selection process (see also Quinn et al., 2009).

If the synchronization terms are dominating the model equations, then the model should be seen as inconsistent with the data. Therefore, they propose the following ratio $R(n)$ with values ranging from $R(n) = 0$ (indicating an inconsistent model) to $R(n) = 1$ (indicating a perfectly consistent model, with $u(n) = 0$ for all n):

$$R^2(n) = \frac{f_1(\mathbf{y}(n), \mathbf{r})^2}{f_1(\mathbf{y}(n), \mathbf{r})^2 + [u(n)(x_1(n) - y_1(n))]^2}. \tag{1.13}$$

Although there is no standard for significance testing or otherwise comparing $R(n)$ values, they will serve as a basic measure of success for the methods developed here. Given that the models tested here have not been independently validated (as validation requires the development of a more robust parameter-selection method in the first place), we will not be able to distinguish model inconsistency from parameter-selection inconsistency. These issues, and others related to model and method assessment, will be examined in more detail in Chapter 6: Conclusions.

Parameter dynamics

Saltzman and Munhall (1992) identify three types of dynamics: state dynamics, parameter dynamics, and graph dynamics. State dynamics refers to change in a system's state; this is the typically what an unqualified "dynamics" refers to. Parameter dynamics refers to change in a system's parameters, and graph dynamics refers to changes in a system's architecture. Here, we are interested in the notion of parameter dynamics, as it can inform us as to the role that parameters can play in behavioral dynamics research.

Parameter dynamics take place on a longer time scale than state dynamics. As mentioned previously, parameter values are invariant within one action "bout", one realization

of the dynamical system. However, they are not necessarily invariant *across* realizations. Changes in parameter values can correspond to changes across development, learning, sensorimotor adaptation, and even changes in context (Saltzman & Munhall, 1992). In this regard, parameter values may actually be of direct interest, as they may track changes over time or over experimental condition. In theory, a behavioral dynamics researcher should be able to use parameter dynamics to measure how the dynamical system has changed across realizations.

Earlier, I speculated as to the reasons why behavioral dynamics models are so rare compared to the attention the theory has received within the perception-action community. I argued that dynamical theory and its relevance to behavior has outpaced the practical realities of model-building in part due to the perception that dynamical models are merely descriptive. However, Saltzman and Munhall's (1992) notion of parameter dynamics may hint at a practical use for models in a traditional, experimental research program. Specifically, I propose that parameters be considered as potential dependent variables for experimental and longitudinal designs. In this way, one could predict specific changes in a system's dynamics as a consequence of experimental manipulation. Ideally, it would be possible to test such parameter-dynamics hypotheses by collecting not a scalar outcome variable for each trial, but rather an entire trajectory. In other words, armed with a model and a series of observed trajectories, the researcher can frame experiments as perturbations of a system's parameter dynamics.

This proposed manipulation and observation of parameter dynamics requires further methodological advancements in the area of parameter selection. We already face the problem of fitting one set of parameters to multiple to trajectories, but now we must also consider the possibility of variation within the parameter set. Therefore, when developing parameter-fitting methods, we should also consider the possibility of allowing certain parameters—

identified by theoretical considerations and/or experimental design—to vary across realizations while holding others constant. Additionally, we must also seek a method for testing hypotheses formulated in terms of parameter dynamics.

In this dissertation, I extend DPE with the goal of embedding traditional regression models into the parameter-selection process. The objective is to allow for parameter values to be a product of fixed and random effects, and to perform hypothesis tests on these effects. I will develop this method in the context of three experiments. The first was originally designed in order to validate the moving-obstacle component of the steering-dynamics model (Bruggeman et al., 2013); Experiments 2 and 3 concern the affordance-based braking model (Harrison et al., 2016).

Chapter 2

General methods

The three experiments described in this dissertation have in common the method of parameter estimation, Multi-Level Dynamical Parameter Estimation (MLDPE), which I will describe in this chapter.

Modifying DPE

DPE (Abarbanel et al., 2009) can be simply modified to allow for multiple observed timeseries. The cost function, Equation 1.12, can be calculated separately for each timeseries, and summed together. Equality constraints, consisting of the model's difference equation with an extended Luenberger observer, can be constructed independently from each series.

Similarly, we can allow for multiple observed dimensions by introducing a multi-dimensional extended Luenberger observer. Thus, we include the synchronization term in the difference equation for each observed dimension, and consider each dimension of the synchronization constant $\mathbf{u}(n)$ in the cost function.

These changes result in a decision vector $\mathbf{x}$ consisting of ND_{model} state values, where N is the total number of observations and D_{model} is the dimensionality of the model; ND_{observed} synchronization strengths, where D_{observed} is the number of observed dimensions (each with an extended Luenberger observer); and P parameters. The resulting optimization problem has $N - M$ equality constraints, where M is the number of observed trajectories.

Hierarchical parameters

The Multi-Level aspect of MLDPE is created by introducing hierarchical parameters. First, consider the possibility of allowing a parameter p to vary by sampling unit (e.g., by participant), creating parameters $p_1, \ldots, p_M$, where M is the number of sampling units. This simply increases the number of parameters in the model.

We can then introduce relationships among the parameters p_m such that

$$p_m = \beta_{p,0} + \epsilon_{p,m}, \tag{2.1}$$

and then treat $\beta_{p,0}$ and $\epsilon_{p,m}, m = 1, \ldots, M$ as first-class parameters in the parameter-selection process, substituting for p_m according to Equation 2.1. This reformulation allows us to include $\epsilon_{p,m}$ in the cost function according to

$$C(\epsilon_{p,1}, \ldots, \epsilon_{p,M}) = \frac{c_p}{2M} \sum_{m=1}^{M} \epsilon_{p,m}^2, \tag{2.2}$$

where c_p is a gain hyperparameter determining how to weigh the cost of parameter error against the other elements of the cost function in Equation 1.12. Thus, the optimization process will seek parameter values that minimize each sampling unit's $\epsilon_{p,m}$. Also, any bound constraints on p become inequality constraints, one for each p_m.

We can further expand Equation 2.1 to include within-subjects effects, and more generally all the elements of mixed-effect regression. For example, if we have predictors Y_q associated with each trial, we can determine parameter values according to

$$p_q = \beta_{p,0} + \beta_{p,Y} Y_q + \epsilon_{p,m}, \tag{2.3}$$

where m is the participant (more generally, the sampling unit) associated with trial q. Any number of fixed effects can be added in this manner according to an arbitrary design matrix.

By including the individual values of β and ϵ as first-class parameters in the optimization decision vector, and penalizing the magnitude of ϵ according to Equation 2.2, we can embed regression-like relationships inside the parameter-selection process.

This is in contrast to a two-step procedure, which might involve fitting each p_k independently and then testing for regression relationships after the fact. Such a method might find no relationship among the parameters when such a relationship really does exist, because the optimization only outputs a single parameter set. If a parameter set exists that includes the hypothesized relationship among the parameter, but only marginally decreases the overall fit, we would consider this a confirmation of the relationship, but the two-step method would not find it. Furthermore, if the hypothesized relationship does in fact exist, by constraining the optimization process accordingly, we hint to the solver what areas of solution space to search, which may improve performance relative to unconstrained parameter relationships.

MLDPE

A full description of the method is as follows:

$$\begin{aligned} \underset{\mathbf{x}}{\text{minimize}} \quad & C(\mathbf{x}) \\ \text{subject to} \quad & g_i(\mathbf{x}) = 0, \\ & h_j(\mathbf{x}) \geq 0, \end{aligned} \tag{2.4}$$

where $\mathbf{x}$ includes state values $\mathbf{y}(n)$, parameter values $\mathbf{r}$, and synchronization gains $\mathbf{u}(n)$. The parameter vector $\mathbf{r}$ includes all β and ϵ values as used in Equation 2.3. The objective function $C(\mathbf{x}) = C(\mathbf{y}(n), \mathbf{r}, \mathbf{u}(n))$ is

$$C(\mathbf{y}(n), \mathbf{r}, \mathbf{u}(n)) = \frac{1}{2N} \sum_{n=0}^{N-1} \left[(x_1(n) - y_1(n))^2 + \sum_{i=1}^{D_{\text{obs.}}} u_i(n)^2 \right] + \sum_p \frac{c_p}{2M} \sum_m \epsilon_{p,m}^2. \tag{2.5}$$

Equality constraint functions $\mathbf{g}(\mathbf{x})$ are the difference equations with observers, Equation 1.11. Inequality constraint functions $\mathbf{h}(\mathbf{x})$ are problem-dependent, and may be used to place bounds on a hierarchical parameter p_k as described above.

Computing

All analysis and modeling was performed using free and open-source software. THe symbolic computing engine SymEngine 0.3.0 (Čertík, Peterson, et al., 2015–), via its Python interface, was used for constructing objective and constraint functions, converting ODEs to difference equations, and differentiating (taking the Jacobians and Hessians) of objective and constraint functions. Optimization problems were constructed using PyGMO the Python interface to the solver library PaGMO 2.4 (Biscani, Izzo, & Yam, 2010) and solved using the

Interior Point Optimization (Ipopt; Wächter & Biegler, 2006) algorithm. A PaGMO population size of 20 was used for all fits. Numerical ODE solutions were estimated using the algorithms in the Fortran library ODEPACK (Hindmarsh, 1983) as exposed in the Python library SciPy (Jones, Oliphant, Peterson, et al., 2001–). Array manipulation of numerical and symbolic objects was done using NumPy (van der Walt, Colbert, & Varoquaux, 2011). Plots were constructed using Matplotlib (Hunter, 2007) and Seaborn (Waskom, Botvinnik, O'Kane, et al., 2017). All analyses were conducted on Google Compute Engine instances.

Chapter 3

Experiment 1: Moving-obstacle avoidance

Due to parameter-selection difficulties, the moving obstacle component of the steering dynamics model remains unpublished (Bruggeman et al., 2013). In the unpublished manuscript, a genetic algorithm was described, but the authors were ultimately unsatisfied with the results. Here, I will how that MLDPE can produce a reasonable parameter fit in much faster time than global methods such as genetic algorithms.

Methods

Participants

Twenty-eight adult undergraduate and graduate Brown University students (thirteen female, fifteen male; ages 18–26) participated in Experiment 1. None reported any visual or motor impairment. They were paid a nominal amount for their participation.

Apparatus

Experiment 1 was conducted in the Virtual Environment Navigation Laboratory (VENLAB) at Brown University, a 12 m × 12 m ambulatory virtual environment. Participants wore a stereoscopic head-mounted display (HMD; Kaiser Electro-Optics Proview 80) with a 60° (horizontal) × 40° (vertical) field of view. Binocular disparity was calculated by measuring the inter-ocular distance of each participant. Virtual environments were generated using the Sense8 World Toolkit software on a graphics workstation (SGI Onyx2); images were presented at 60 frames per second. Participants' position and orientation were measured using a hybrid ultrasonic-inertial tracking system (Intersense IS-900) with six degrees of freedom at 60 Hz, and used to update the display with a latency of approximately 70 ms (4 frames).

Displays and environment

The virtual environment consisted of a textured ground plane (50 m^2) and a black sky. The ground texture map was made up of randomly generated grayscale squares. A goal (blue pole) was positioned at 7.0 m from the starting location (specified by a multicolored pole), with an orientation marker (red pole) in-between. The obstacle (yellow pole) moved across the participant's path on various trajectories (see Figure 3.2). All poles were granite-textured vertical cylinders with a radius of 1 m; the start, orientation, and target poles were 2.5 m (approximately 1.5 eye heights) tall and the obstacle pole was 2.0 m (approximately 1.2 eye heights) tall. Figure 3.1 shows a screenshot from the experiment.

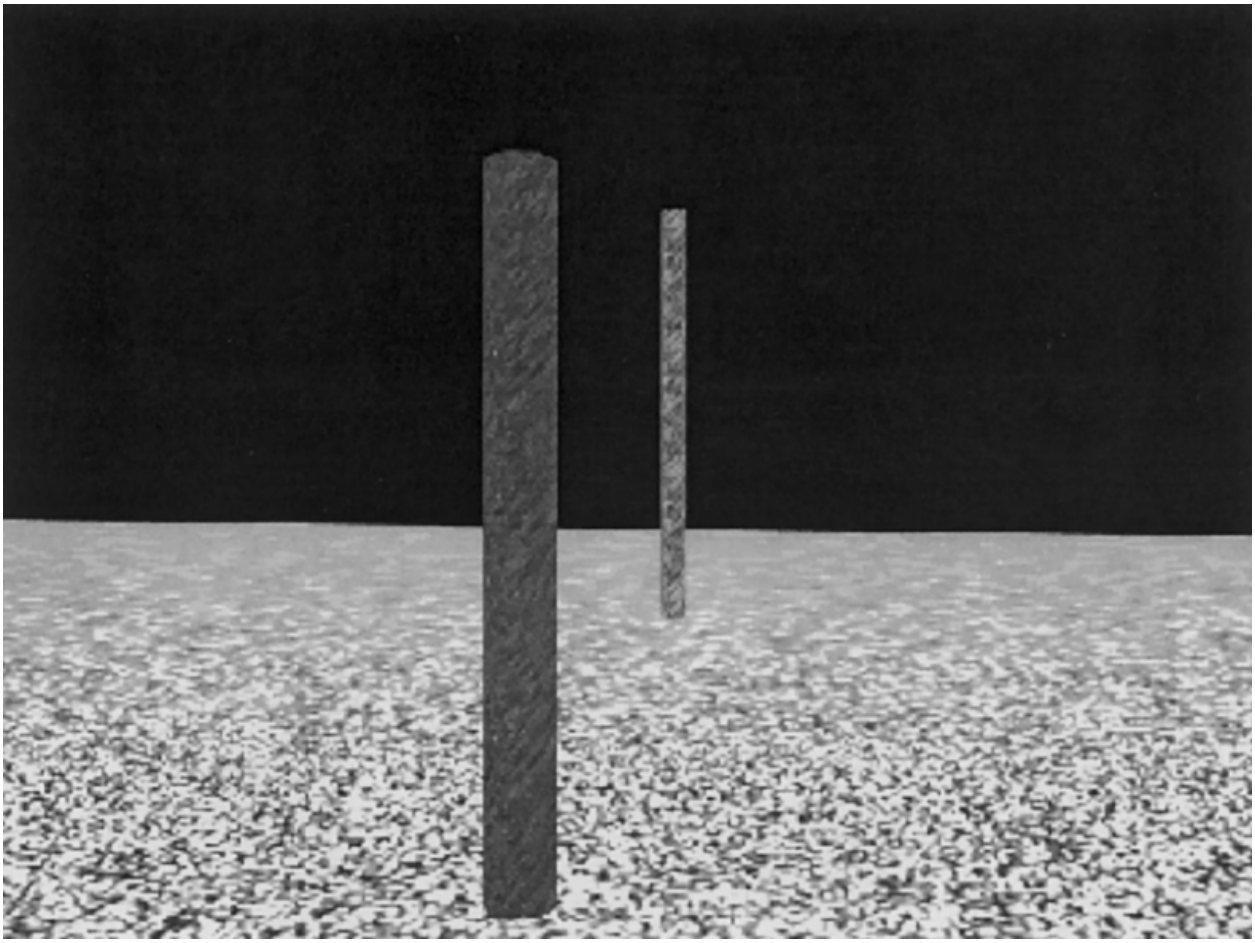

FIGURE 3.1: Screenshot from Experiment 1, showing the goal and obstacle poles (reproduced in grayscale).

Procedure

Prior to each trial, with only start and orientation poles visible, participants were instructed to position themselves at the starting location and face the orientation marker. Trials began when the orientation pole disappeared, signaling that the participant should begin walking forward toward its position. After walking one meter, the goal and obstacle poles appeared. This procedure ensured that participants obtained a steady-state walking speed and heading direction which would define initial conditions for subsequent modeling. Participants were instructed to walk at a comfortable speed to the goal while steering to avoid the moving obstacle. When they walked into the goal it disappeared, the trial ended, and the start and orientation poles reappeared for the next trial. If the participant walked too close to the obstacle pole (within 15 cm), a collision sound was heard and the event was recorded. Participants were informed that they could take a break or discontinue the experiment; all participants completed the experiments without incident. The research protocol was approved by Brown University's Institutional Review Board.

Design

This experiment was originally designed as two experiments. For the purpose of this dissertation, data were analyzed together; nevertheless, we will describe the designs separately.

Design 1A

Fourteen participants participated in Experiment 1A. Figure 3.2A illustrates the conditions of this design. Obstacle speed and obstacle trajectory were manipulated, such that each obstacle always crossed the depth (z) axis between the start and goal poles at a point 3.7 m from the starting location. The obstacle's motion varied among three trajectories, which were

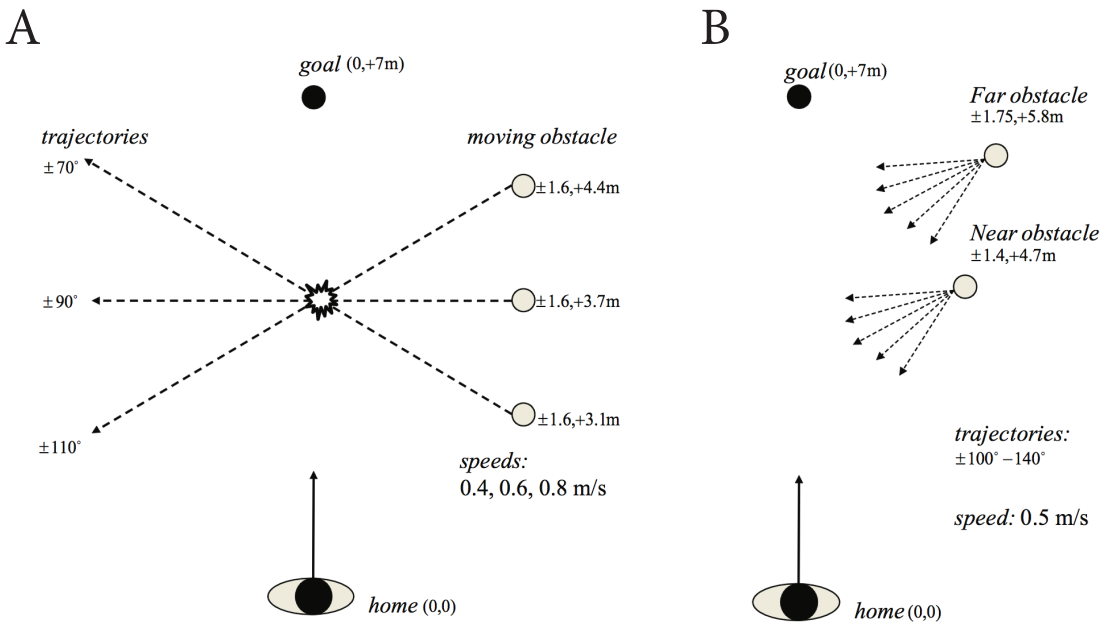

FIGURE 3.2: Top-down view of the design of Experiment 1.

reflected about the z axis (70, 90, 110° with respect to the z axis) and three speeds (0.4, 0.6, 0.8 m/s), creating a 3 (trajectory) × 3 (speed) design. The obstacle's initial position with respect to the starting location was $x = 1.6$ m, $z = 3.1$, 3.7, or 4.4 m, respectively, for motion along a 70, 90, or 110° trajectory. Each participant completed eight trials in each condition, for a total of 72 trials. Trials were presented in nine blocks with a complete set of conditions per block, in a randomized order within blocks.

Design 1B

Fifteen participants participated in Experiment 1B. Figure 3.2B illustrates the conditions of this design. The collision point of the obstacle was manipulated by varying the obstacle's initial distance and trajectory, while holding its speed constant. There were five different obstacle trajectories, which were reflected about the z axis (100, 110, 120, 130, 140°), and

two initial distances (4.7, 5.8 m), creating a 5 (trajectory) $\times$ 2 (distance) design. Obstacle speed was held constant at 0.5 m/s. The near obstacle had an initial position of $x = 1.4$ m, $z = 4.7$ m and the far obstacle had an initial position of $x = 1.75$ m, $z = 5.8$ m. Each participant completed 60 trials in 10 blocks of 6 trials each; order of the trials was randomized within blocks.

Data analysis

The two-dimensional coordinates of head position were recorded to disk at a sampling rate of 30 Hz. These data were filtered using a forward and backward 4th-order Butterworth filter with a cutoff frequency of 0.6 Hz, to reduce noise due to head and gait oscillations. Data for leftward and rightward trajectories were collapsed prior to further analysis. Trials were cropped at the moment the participant crosses the obstacle's trajectory.

Model

The full model used for this experiment includes the stationary goal term (Equation 1.2) and a moving obstacle term (Equation 1.5) in the heading ODE, while Equation 1.6 is used as

the speed ODE. As a series of first-order ODEs, we arrive at the seven-dimensional system

$$\begin{aligned}
\dot{y_1} &= \ddot{\phi} = -b_{\mathrm{g}}\dot{\phi} - k_g\beta_{\mathrm{g}}(e^{-c_1 d_{\mathrm{g}}} + c_2) + k_{\mathrm{mo}}(-\dot{\psi}_{\mathrm{o}})e^{-c_5|\dot{\psi}_{\mathrm{o}}|}e^{-c_6 d_{\mathrm{o}}} \\
\dot{y_2} &= \dot{\phi} \\
\dot{y_3} &= \dot{v} = b_v(v - v_{\mathrm{p}}) + k_v\dot{\psi}_{\mathrm{o}}(\operatorname{sgn}\dot{\psi})e^{-c_7|\dot{\psi}_{\mathrm{o}}|}e^{-c_8 d_{\mathrm{o}}} \\
\dot{y_4} &= \dot{x} = v\cos\phi \\
\dot{y_5} &= \dot{z} = v\sin\phi \\
\dot{y_6} &= \dot{x}_{\mathrm{o}} = v_{\mathrm{o}}\cos\phi_{\mathrm{o}} \\
\dot{y_7} &= \dot{z}_{\mathrm{o}} = v_{\mathrm{o}}\sin\phi_{\mathrm{o}},
\end{aligned} \tag{3.1}$$

where (x, z) is the agent's (participant's) location and $(x_{\mathrm{o}}, z_{\mathrm{o}})$ is the obstacle's location. Obstacle speed v_{o} and heading ϕ_{o} are determined in advance by the experimental condition. Notice that Equation 3.1 does not include the sign modifier (cf. Equation 1.6). It has marginal impact due to the cropping of the trials (see previous section) and removing discontinuities aids the fitting process.

The rate of change of obstacle-bearing angle $\dot{\psi}_{\mathrm{o}}$ can be expressed as a function of $\mathbf{y}$ (Fajen & Warren, 2007):

$$\dot{\psi}_{\mathrm{o}} = \frac{(z_{\mathrm{o}} - z)(\dot{x}_{\mathrm{o}} - \dot{x}) - (x_{\mathrm{o}} - z)(\dot{z}_{\mathrm{o}} - \dot{z})}{(x_{\mathrm{o}} - x)^2 + (z_{\mathrm{o}} - z)^2}, \tag{3.2}$$

as can d:

$$d_n = \sqrt{(x_n - x)^2 + (z_n - z)^2}. \tag{3.3}$$

Parameter selection

MLDPE was used for parameter selection, with v_{p} allowed to vary per participant according to Equation 2.1, with no fixed effects. The parameters relating to the moving-goal component

of the model were set to b_{g}, k_{g}, c_1, and c_2 were set to the values reported in the Introduction (see Steering dynamics model), from Warren and Fajen (2008). The state dimensions heading ϕ and state v were treated as observed.

Due to efficiency limitations, a random subset of 112 trials was used for MLDPE. For the same reason, observed trajectories were resampled at 0.5 Hz before analysis.

Results

Parameter selection

Ipopt failed to converge on a solution to the optimization problem; it terminated due to reaching the maximum number of function evaluations (10,000). Nevertheless, the best-fitting parameter values out of all tested values was reported. The resulting parameter values are shown in Table 3.1.

The timeseries of consistency ratios $R^2(n)$ is shown in Figure 3.3. The overall median ratio was $1 - 1.63e^{-11}$, and the minimum was $1 - 6.24e^{-6}$, indicating extremely high model consistency for all n. Because these values are so close to 1, the underlying synchrony coefficients $u(n)$ are also shown in Figure 3.3. As there are two observed dimensions, there are two observed series of synchrony coefficients.

Discussion

Several aspects of the selected parameter set are notable. The most striking result is the very low values of the preferred speed errors $\epsilon_{v_{\mathrm{p}}}$ and preferred-speed coefficient b_v. Thus, the optimizer found a creative way to minimize the cost function: by reducing b_v nearly to zero,

Param.	Value
k_{o}	199.053
c_5	31.355
c_6	0.1303
b_v	0.0021
k_v	38.320
c_7	17.733
c_8	13.471
$\beta_{v_{\mathrm{p}},0}$	11.883
$\epsilon_{v_{\mathrm{p}},1}$	−0.00170
$\epsilon_{v_{\mathrm{p}},2}$	−0.00163
$\epsilon_{v_{\mathrm{p}},3}$	−0.00222
$\epsilon_{v_{\mathrm{p}},4}$	0.00015
$\epsilon_{v_{\mathrm{p}},5}$	0.00062
$\epsilon_{v_{\mathrm{p}},6}$	−0.00168
$\epsilon_{v_{\mathrm{p}},7}$	−0.00104
$\epsilon_{v_{\mathrm{p}},8}$	0.00214
$\epsilon_{v_{\mathrm{p}},9}$	0.00028
$\epsilon_{v_{\mathrm{p}},10}$	0.00524
$\epsilon_{v_{\mathrm{p}},11}$	−0.00202
$\epsilon_{v_{\mathrm{p}},12}$	0.00049
$\epsilon_{v_{\mathrm{p}},13}$	−0.00294
$\epsilon_{v_{\mathrm{p}},14}$	−0.00118
$\epsilon_{v_{\mathrm{p}},15}$	−0.00079
$\epsilon_{v_{\mathrm{p}},16}$	0.01414
$\epsilon_{v_{\mathrm{p}},17}$	−0.00140
$\epsilon_{v_{\mathrm{p}},18}$	−0.00109
$\epsilon_{v_{\mathrm{p}},19}$	0.00116
$\epsilon_{v_{\mathrm{p}},20}$	0.00276
$\epsilon_{v_{\mathrm{p}},21}$	0.00330
$\epsilon_{v_{\mathrm{p}},22}$	0.00753
$\epsilon_{v_{\mathrm{p}},23}$	−0.00084
$\epsilon_{v_{\mathrm{p}},24}$	−0.00963
$\epsilon_{v_{\mathrm{p}},25}$	−0.00432
$\epsilon_{v_{\mathrm{p}},26}$	−0.01331
$\epsilon_{v_{\mathrm{p}},27}$	−0.00165
$\epsilon_{v_{\mathrm{p}},28}$	−0.00543

TABLE 3.1: Parameter values selected by MLDPE for Experiment 1.

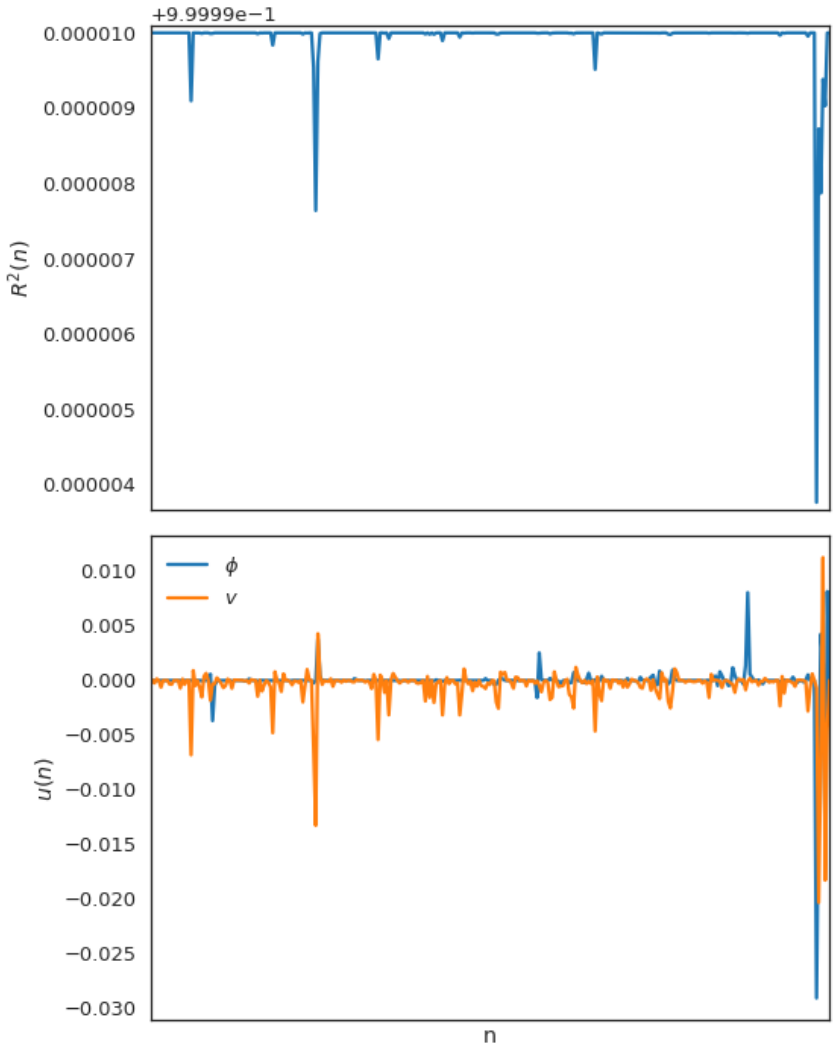

FIGURE 3.3: Consistency ratio $R^2(n)$ (top) and synchrony coefficients $u(n)$ (bottom) for Experiment 1. Note the y-axis—the range of $R^2(n)$ was extremely small.

then it could also reduce the errors while minimally impacting the model fit. This suggests that the trade-off between synchronization error and parameter error needs to be further examined.

Additionally, MLDPE selected a large value of c_7, the distance modifier for speed control, that effectively canceled out the entire constant-bearing angle acceleration term. Therefore, simulated agents accelerated at a nearly constant speed at every trial, not adhering to the constant-bearing angle strategy. This can be observed in the representative trial shown in Figure 3.4

Given this pattern of results, it appears that the parameter selection for the speed-control term was unsuccessful. This could be because the model is incorrectly specified; however Bruggeman et al. (2013) did observe a pattern of accelerations and decelerations consistent with using speed to control bearing angle. An alternative explanation is that the assumptions necessary for Ipopt to converge (Wächter & Biegler, 2006) did not hold. Specifically, the constraint functions were not twice differentiable, owing to the absolute value and sign functions in the model equation. The use of circular arithmetic and modulus functions, necessary due to the formulation of the problem in terms of angular acceleration, may have also created irregularities in the problem's Jacobian and Hessian functions.

The modulus-function issue could be solved by implementing proper circular arithmetic handling in the symbolic computation library (symengine; Čertík et al., 2015–) that was used to create the problem functions and differentiate them. However, the lack of compatibility with absolute values and sign functions may be an insurmountable drawback of local search methods. If the search space and problem constraints are not smooth, the algorithm cannot leverage the Jacobians and Hessians and therefore may not converge. In this case, global optimization may be the only feasible recourse.

Finally, consistency ratios $R^2(n)$ very close to unity were observed, despite the clear

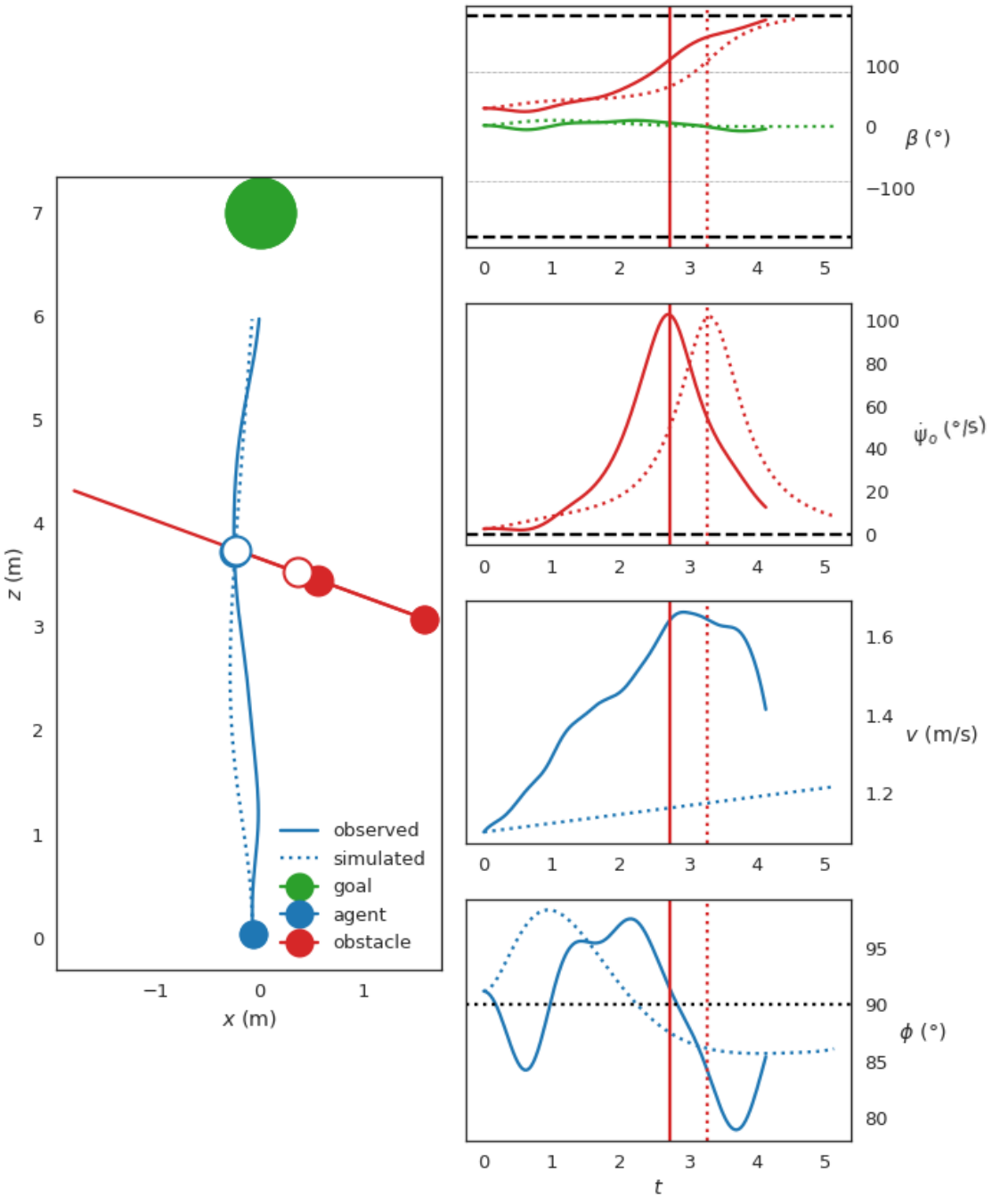

FIGURE 3.4: An example trial from Experiment 1, including a simulated trajectory using the selected parameter values. Left: birds-eye view of the observed (solid) and simulated (dotted) trajectories. The location of the agent and obstacle at the time that the agent crossed the obstacle trajectory is shown with filled (observed) and open (simulated) circles.
Right: timeseries of variables relevant to each trajectory and the model, for both observed (solid) and simulated (dotted) trajectories. Right vertical lines indicate the time at which each agent crossed the obstacle's trajectory. Two pairs of series are drawn in the β panel (top); green refers to β_g and red to β_o.

inconsistency in the model's treatment of agent speed. This casts doubt on the suggestion in Abarbanel et al. (2009) that this is an indication of model consistency. It may be impacted by the scale of the state variables; in this case in particular it could be caused by modulus arithmetic, because the consistency ratio when $\phi = \pi$ will be lower than when $\phi = 3\pi$, despite these cases being equivalent. Thus, it is clear that circular arithmetic poses a problem that is not unique to MLDPE but also applies to the original method, DPE.

Chapter 4

Experiment 2: Braking in behavioral contexts

Whereas the modeling in Experiment 1 allowed for a parameter to vary by sampling unit (participant), with Experiment 2 we will also allow parameters to vary by experimental condition. The behavioral dynamics of affordance-based control (Harrison et al., 2016) imply that soft constraints, including contextual factors, are required to determine the actual path taken through Fajen's (2007) safe zone. In Experiment 2, participants were placed in emergency braking situations in two contexts: a race and a safety test. The affordance-based behavioral dynamics perspective predicts that we should observe a difference in soft constraints between these two contexts. We will use MLDPE to look for systematic differences in parameter values depending on this experimental condition of instructional context. Specifically, we expect that participants in the race condition will exhibit behavior consistent with preferring faster steady-state speeds, manifesting as greater values of the parameter preferred velocity v_{p}.

Methods

Participants

Eight undergraduate and graduate University of Connecticut students participated in this experiment (5 female, 3 male; ages 19–29). All were licensed to drive in United States. Undergraduate participants received course credit in exchange for their participation. The research protocol was approved by the University of Connecticut's Institutional Review Board.

Apparatus

Experiment 2 was conducted in a driving simulator. Participants controlled the virtual vehicle using Fanatec ClubSport Pedals V2 (Endor AG). Only the accelerator and brake pedals were used; the virtual vehicle had an automatic transmission, and so the clutch pedal was not connected. Participants held a Fanatec ClubSport Porsche 918 RSR Wheel (Endor AG) although the wheel was not connected to the display. Displays were generated using the Unity 3D game engine (Unity Technologies) and displayed on a 28 in. IPS display (Dell, Inc.) at a frame-rate of approximately 60 Hz. Vehicle physics were implemented using the Unity package Vehicle Physics Pro (vehiclephysics.com). This created a highly realistic driving experience, including a tire friction model, air drag, and automatic transmission.

Displays and environment

Figure 4.1 shows a screenshot from Experiment 2. The virtual environment consisted of an asphalt road extending straight into the horizon. The road had a width of approximately 5 vehicle widths; it had a dashed white dividing line and the vehicle drove on the right-

FIGURE 4.1: A screenshot from Experiment 2, showing the cabin view, road, grass area, trees, stop sign, and stopping area.

hand side of the road. The road was flanked by a green grass texture to the horizon; the environment outside the road was filled with randomly placed trees. Participants drove a virtual pickup truck, and viewed the environment from the perspective of inside the cabin, with view of the speedometer and engine RPM display. Periodically (see Procedure), a stop sign would appear directly in the vehicle's path. The stop sign had a width of approximately half the vehicle's width, and was centered at the driver's eye position. In front of the stop sign, a rectangular area of the road was colored a light gray, indicating the area in which the driver should stop. The stopping area extended 3 vehicle lengths in front of the stop sign.

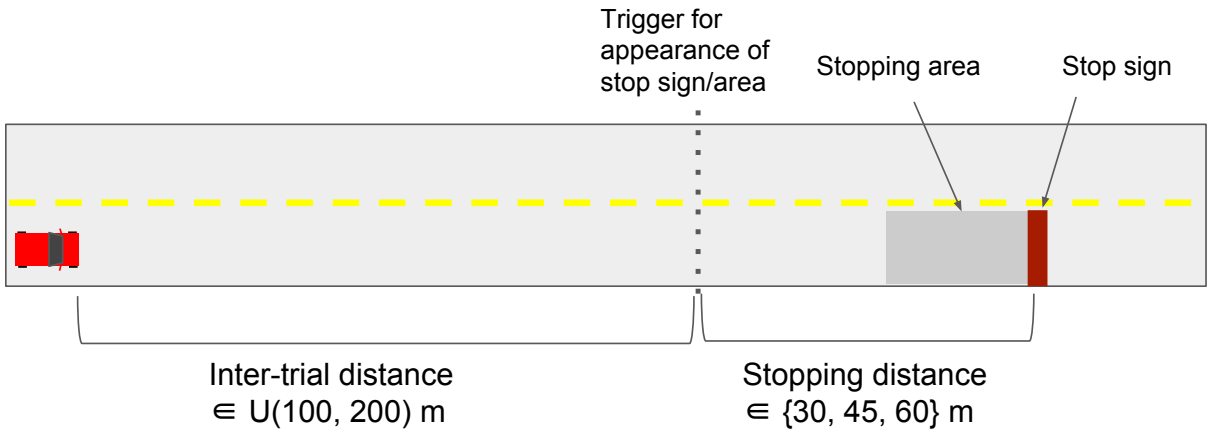

FIGURE 4.2: An overview of the course of events during a trial in Experiment 2.

Procedure

Each block of trials began by showing a third-person perspective from the outside the vehicle, in order to show the participant the vehicle and its placement within the environment. When the participant was ready to begin, a key was pressed on the keyboard, moving the camera to inside the vehicle as in Figure 4.1. The participant was instructed to accelerate to a comfortable pace. Trials were triggered after the participant had driven a certain distance, selected randomly between 100 and 200 m. When a trial was triggered, the stop sign appeared suddenly in the road. The participant was instructed to come to a stop, remain inside the marked stopping area until the stop sign disappeared, and then to continue driving. After each sequence of stop signs was encountered, the environment was reset, the display switched to the third-person perspective, and the environment frozen while the participant was given an opportunity to take a break from the experiment. The sequence of events within each trial are shown in Figure 4.2.

After the first block, participants were given additional instructions. Participants in the race condition were told that they should complete the course as fast as possible without

colliding with the stop signs, and that their times would be compared with those of other participants. Participants in the safety-test condition were told that they were being tested on their safety, and that they would be compared against other participants in terms of how smooth their driving habits were.

Design

Within-subject independent variables were distance between the driver and stop sign at trial start, and time in the stopping area until the stop sign disappeared. Between-subject independent variables were maximum brake torque and behavioral context. There were three stopping distances (30, 45, 60 m), three stop times (1, 3, 5 s), two maximum brake torques (2000, 6000 Nm), and two behavioral contexts (race, safety test), creating a $3 \times 3 \times 2 \times 2$ design. Each block contained a full cross of the within-subject independent variables, with each condition repeated twice, for a total of 18 trials. After the training block, each participant completed four further blocks for a total of 72 trials.

Data analysis

Data was recorded from the Vehicle Physics telemetry module at every frame. Recorded data included the position of the vehicle and the state of vehicle components include pedal positions. Data was resampled at 2 Hz using linear interpolation when necessary. For analysis, trials were cropped from the time the obstacle appeared until the participant came to a complete stop (if the participant came to a complete stop more than once during a trial, the trial was cropped at the time of the final stop).

Model

The full model is Equation 1.7 expressed a system of first-order ODEs:

$$\begin{aligned} \dot{y_1} &= \dot{a} = -b(v - v_{\mathrm{p}}) - k\left(\frac{a - a_{\mathrm{ideal}}}{a_{\mathrm{ideal}} - a_{\mathrm{min}}}\right) \\ \dot{y_2} &= \dot{v} = a \\ \dot{y_3} &= \dot{x} = v. \end{aligned} \tag{4.1}$$

Ideal acceleration a_{ideal} can be determined as a function of $\mathbf{y}$ by the equation (Harrison et al., 2016):

$$a_{\mathrm{ideal}} = \frac{v^2}{2x}. \tag{4.2}$$

For current purposes, a_{min} can be predetermined in advance of simulation or parameter selection from the parameters of the vehicle simulator (maximum brake torque, wheel radius, and vehicle mass).

Parameter selection

MLDPE was used to select parameter values, with position x and speed v treated as observed dimensions. Preferred velocity v_{p} was allowed to vary per participant according to Equation 2.1 with an intercept $\beta_{v_{\mathrm{p}},0}$ and a fixed effect $\beta_{v_{\mathrm{p}},1}$ for condition, allowing for different values of v_{p} by condition as well as participant. This fixed-effect was coded such that it took a value of 0 in the safety condition and 1 in the race condition. That is, in the safety condition $v_{\mathrm{p},m} = \beta_{v_{\mathrm{p}},0} + \epsilon_{v_{\mathrm{p}},m}$ and in the race condition, $v_{\mathrm{p},m} = \beta_{v_{\mathrm{p}},0} + \beta_{v_{\mathrm{p}},\mathrm{race}} + \epsilon_{v_{\mathrm{p}},m}$. Inequality constraints were added to the optimization problem of the form $a(n) \geq a_{\mathrm{min}}$, with the values of a_{min} specific to the brake-strength condition of each trial. Due to efficiency and memory limitations, only data from four participants was analyzed (288 trials total), two

Param.	Value
k_a	5.713
k_v	0.167
$\beta_{v_\mathrm{p},0}$	3.602
$\beta_{v_\mathrm{p},\mathrm{race}}$	3.092
$\epsilon_{v_\mathrm{p},1}$	3.097
$\epsilon_{v_\mathrm{p},2}$	−3.097
$\epsilon_{v_\mathrm{p},3}$	−1.775
$\epsilon_{v_\mathrm{p},4}$	1.775
$v_{\mathrm{p},1}$	9.791
$v_{\mathrm{p},2}$	3.597
$v_{\mathrm{p},3}$	1.827
$v_{\mathrm{p},4}$	5.378

TABLE 4.1: Parameter values selected by MLDPE for Experiment 2. Values of v_p were reconstructed according to Equation 2.1.

from each condition.

Results

Parameter selection

Ipopt successfully converged on a solution to the optimization problem. The resulting parameter values are shown in Table 4.1. Given that $\beta_{v_\mathrm{p},\mathrm{race}} = 3.092$, MLDPE found that preferred velocity v_p was higher in the race condition, as expected. However, we have no way of judging whether this effect is "significant" (see Conclusions), and the reconstructed values of v_p are unconvincing as to the size of this effect. Additionally, note that parameter values for participants in the same condition are equally spaced from the condition mean. This provides some confidence that the hierarchical parameter error cost (Equation 2.2) is working as intended.

The timeseries of consistency ratios $R^2(n)$ is shown in Figure 4.3. The overall median

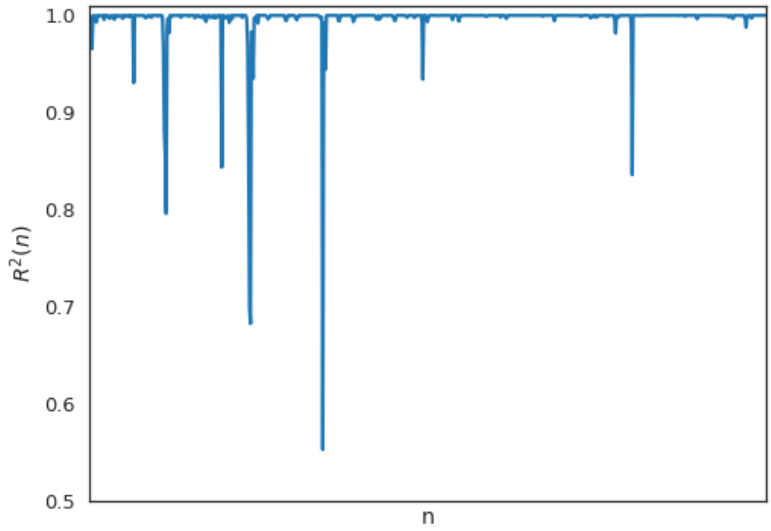

FIGURE 4.3: Consistency ratio $R^2(n)$ for Experiment 2.

ratio was 0.99985, indicating high model consistency. However, dramatic drops in model consistency were observed in seven trials. Nevertheless, the minimum median model consistency of any single trial was 0.992; only three trials had a median model consistency less than 0.999. Thus, we can conclude that the affordance-based braking model is consistent with observed trajectories. Representative observed and simulated trajectories are shown in Figure 4.4.

Safety-margin analysis

Because the difference in model parameters v_{p} is somewhat inconclusive, I also performed a safety-margin analysis. Under the original affordance-based control framework proposed by Fajen (2007), any trajectory that remains within the safe zone is sufficient. However, the safety margin that is actually realized should depend on contextual factors such as the

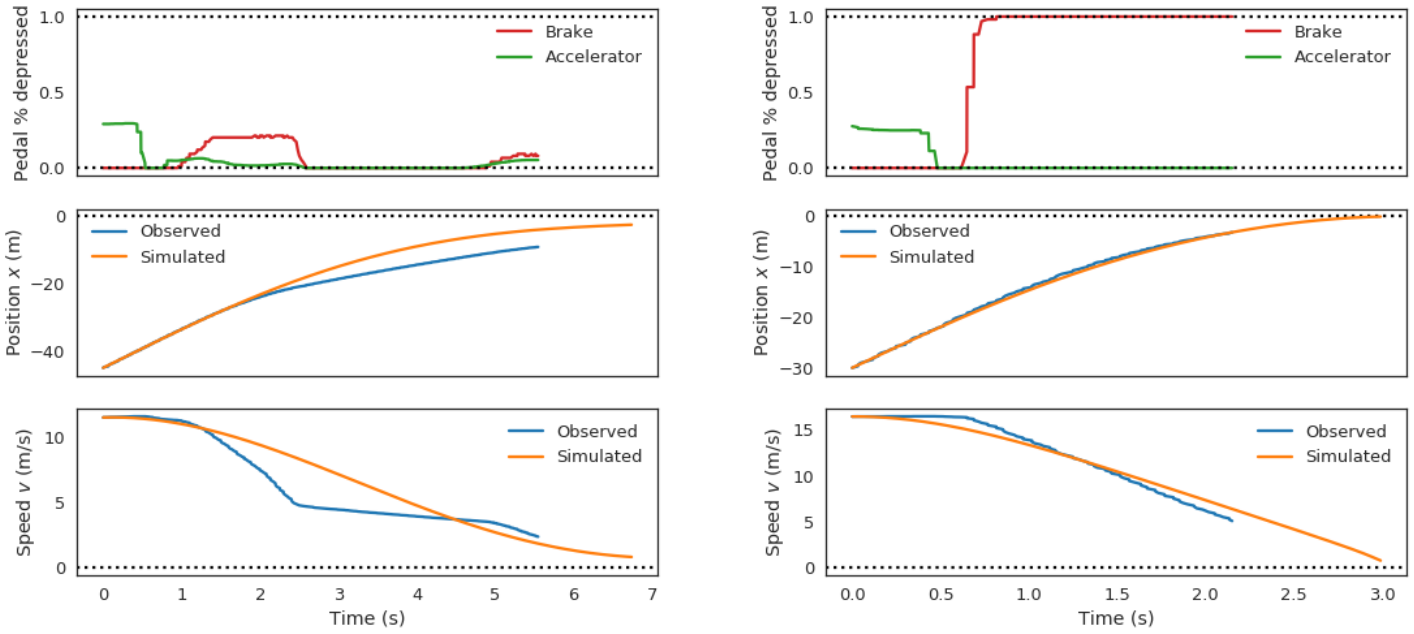

(A) A representative trial from the safety condition, with slight deceleration and coasting.

(B) A representative trial from the race condition, with emergency braking.

FIGURE 4.4: Timeseries from two representative trials from Experiment 2. The top panel in each subfigure shows the observed brake and accelerator pedal depression timeseries; there is no equivalent for the simulated trials. The other panels show both the observed trajectory, and a simulated trajectory. The simulated trajectories are numerical solutions of Equation 4.1, using initial conditions from the observed data and parameter values from the MLDPE fit.

instruction condition in this experiment. This issue is discussed in detail in (Harrison et al., 2016).

With respect to the braking model, the safety margin can be calculated as the maximum velocity, as a function of the participant's current position, at which $a_{\text{ideal}} \geq a_{\text{min}}$. If the participant's speed reaches the safety margin, they must decelerate at full strength to avoid a collision. If the participant's speed exceeds the safety margin, a collision is inevitable.

For the safety-margin analysis, the minimum safety margin was determined for each trial. Safety margins were significantly larger in the safety condition ($M = 9.37$ m/s, $SD = 2.38$ m/s) than in the race condition ($M = 4.22$ m/s, $SD = 3.08$ m/s), $t(106) = 13.75$, $p < .001$. As expected, the context of the experiment determined the participants' trajectories through the safe zones.

Discussion

Although the model does a reasonable job at matching the velocity profiles as the driver decelerates to a stop, it cannot capture all the idiosyncrasies that occur in human driving behavior. Some of these arise from the peculiarities of vehicular locomotion. For example, the model predicts changes in acceleration—positive or negative. However, in an automobile, acceleration and deceleration are a function of two separate pedals, as well as the physical forces on the vehicle such as friction and drag. For a discussion of the consequences of these differences, see (Harrison et al., 2016). For present purposes, a comparison of the velocity profiles suffices, and in this regard the model captures variations in the overall urgency of braking due to differences in initial conditions, vehicle dynamics (i.e., a_{min}), and experimental context.

Regarding the experimental manipulation, the safety-margin analysis shows that it had an impact on participants' trajectories. However, whether MLDPE was able to cache this difference in terms of changes in parameter values is uncertain. In part, this is because confidence intervals could not be constructed around the parameter estimates (see Limitations). This may also be due to a limitation of the model itself: like the behavioral dynamics models it is based on, it assumes that the driver will come to a stop at the exact x location of the obstacle. That is, it cannot account for human drivers' tendency to stop in advance of obstacles. This is an aspect of braking behavior that needs to be tackled from an affordance-based perspective (Harrison et al., 2016) and is out of scope of this dissertation.

Experiment 2 established the feasibility of searching for systematic variation in parameters. Experiment 3 will test the same procedure using the same model, but with an experimental manipulation that has been extensively studied.

Chapter 5

Experiment 3: Braking while distracted

Experiment 2 demonstrated the feasibility of using MLDPE to it parameters while allowing for differences between experimental conditions. Experiment 3 is designed to further validate the method by applying to an experimental manipulation with known results. For this purpose, an experiment testing the effect of distraction while driving is suitable, as the same model can be used as in Experiment 2, in a well-studied context. Hancock, Lesch, and Simmons (2003) tested drivers in a real driving situation under a number of distraction conditions. Here, we applied one of their manipulations, a numeric recall task timed to coincide with a braking event. MLDPE was used to determine how the distractor task affected the dynamics of driving. The results were then compared to the original findings (Hancock et al., 2003) in a general sense. Specifically, given that Hancock et al. (2003) found increased brake response times and stopping times in the presence of a distractor task, we predict a weaker attractor strength for braking. This would manifest as a smaller value of the parameter k_a in the distractor condition.

Methods

Participants

Ten undergraduate University of Connecticut students participated in this experiment (5 female, 5 male; ages 18–21) in exchange for course credit. All were licensed to drive in United States. The research protocol was approved by the University of Connecticut's Institutional Review Board.

Apparatus

Apparatus was the same as in Experiment 2, with the addition of a numeric keypad placed near the steering wheel, which the participant used to respond to the distractor prompts. The lower-left button was colored green and the lower-right button colored red, for responses of "correct" and "incorrect", respectively.

Displays and environment

Displays and environment were the same as in Experiment 2, with the addition of an image of the numeric keypad that was always present on the bottom-right of the screen. An LCD screen was drawn above the keypad to simulate a calculator-like display.

Procedure

The procedure was similar to that of Experiment 2, with several additions after the first practice block, designed to mimic the recall task from Hancock et al. (2003). At the beginning of each block of trials, a seven-digit number was shown in the LCD display. Participants

were told to memorize the number, which disappeared as soon as they initiated the block. A recall task was presented to the participants on half the trials in each block. In these trials, the participant heard a beep between 0.5 and 1 s before the stop sign appeared. At this time, a digit appeared in the LCD display, along with underscores to make apparent its position in the original seven-digit number. Participants were instructed to press the green button if the digit matched the original number, and the red button if it did not. For example, if the original number was "1 2 3 4 5 6 7" and the recall prompt was "_ _ _ _ _ 6 _", the correct response would be to press the green button. Participants were instructed to make the response as soon as possible after hearing the beep, and to keep both hands on the steering wheel when not responding to the recall prompt.

Design

There were two maximum brake torques (3000, 5000 Nm), four stopping distances (20, 30, 40, 50 m), and two distractor conditions (distractor, no distractor). Every block included a full cross of the distractor and stopping-distance variables, with two repetitions of each condition, for a total of 16 trials. Maximum brake torque was varied by block, with each participant experiencing five blocks at each brake torque, for a total of ten blocks (160 trials), not including the practice block.

Data analysis

Data analysis was the same as for Experiment 2.

Model

The model was the same as for Experiment 2.

Parameter selection

Parameter selection was the same as for Experiment 2, except that the fixed-effect of condition on v_{p} was removed. Instead, the braking stiffness parameter k_a was allowed to vary, with a within-subjects fixed-effect of distractor condition. This fixed-effect was coded such that it took a value of 0 in the no-distractor condition and 1 in the distractor condition. That is, in the no-distractor condition $k_a = \beta_{k_a,0} + \epsilon_{k_a,m}$ and in the distractor condition, $k_a = \beta_{k_a,0} + \beta_{k_a,\mathrm{dist.}} + \epsilon_{k_a,m}$

Results

Replication

Two patterns of findings from Hancock et al. (2003) were compared to the current data: stopping time and response time. Hancock et al. (2003) found that distraction caused a slight decrease in stopping time in younger drivers and a larger decrease in older drivers. The effect of distraction on stopping times in the current experiment was tested using a repeated-measures ANOVA. Stopping times were significantly shorter in the distractor condition ($M = 4.04$ s, $SD = 1.54$ s) than in the no-distractor condition ($M = 4.27$ s, $SD = 1.31$ s), $F(1, 20) = 7.556$, $p < .05$. Thus, the finding of a small decrease in stopping times was replicated. Stopping times by condition are shown in Figure 5.1.

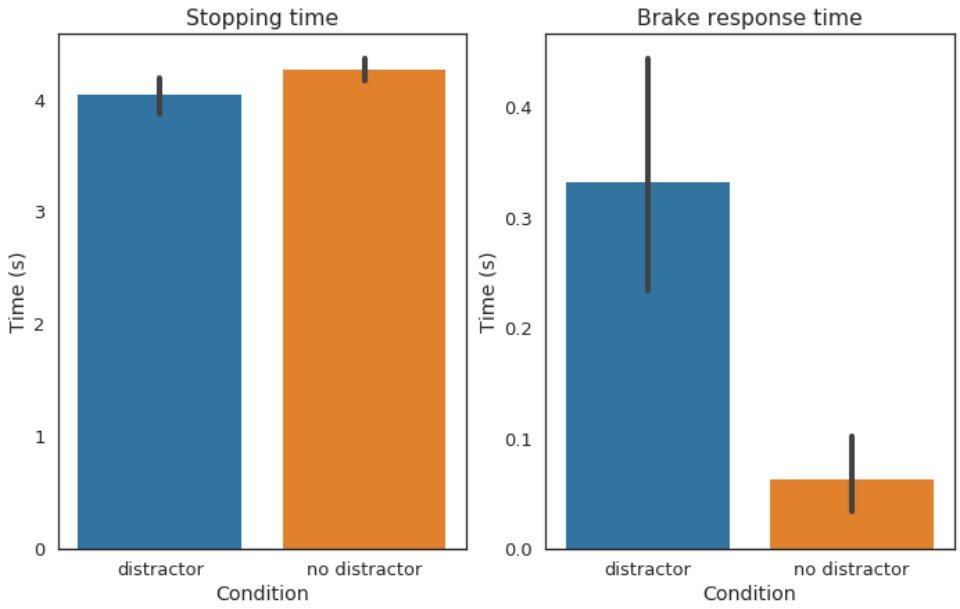

FIGURE 5.1: Stopping times and brake response times by condition in Experiment 3.

Hancock et al. (2003) also found delayed reaction times under distraction conditions. This effect was tested for the current experiment using a repeated-measures ANOVA. Response times were significantly longer in the distraction condition ($M = 0.332$ s, $SD = 1.09$ s) than in the no-distractor condition ($M = 0.063$ s, $SD = 0.46$ s), $F(1, 20) = 7.478$, $p < .05$. Thus, the original findings were replicated. This pattern of results is shown in Figure 5.1.

Parameter selection

Ipopt successfully converged on a solution. The resulting parameter values are shown in Table 5.1. The regression coefficient for the distractor condition $\beta_{k_a,\text{dist.}}$ was -1.454, indicating smaller values of k_a in the distractor condition compared to the no-distractor condition. This difference occurred while also allowing k_a vary by participant according to $\epsilon_{k_a,m}$.

The timeseries of consistency ratios $R^2(n)$ is shown in Figure 5.2. The overall median ratio was 0.99989, indicating high model consistency. However, the trial-by-trial consistency

Param.	Value
k_v	0.1967
v_p	6.857
$\beta_{k_a,0}$	7.493
$\beta_{k_a,\mathrm{dist.}}$	−1.454
$\epsilon_{k_a,1}$	0.0368
$\epsilon_{k_a,2}$	0.0109
$\epsilon_{k_a,3}$	−0.0215
$\epsilon_{k_a,4}$	−0.0169
$\epsilon_{k_a,5}$	0.0307
$\epsilon_{k_a,6}$	−0.0225
$\epsilon_{k_a,7}$	0.0275
$\epsilon_{k_a,8}$	−0.0150
$\epsilon_{k_a,9}$	−0.0358
$\epsilon_{k_a,10}$	−0.0069
$\epsilon_{k_a,11}$	0.0053
$\epsilon_{k_a,12}$	0.0181
$\epsilon_{k_a,13}$	0.2166
$\epsilon_{k_a,14}$	0.0297
$\epsilon_{k_a,15}$	0.0195
$\epsilon_{k_a,16}$	−0.0178

TABLE 5.1: Parameter values selected by MLDPE for Experiment 3. Note that values of b_a could not be reconstructed on a per-participant basis (cf. Table 4.1), because the fixed-effect of condition was a within-subjects variable.

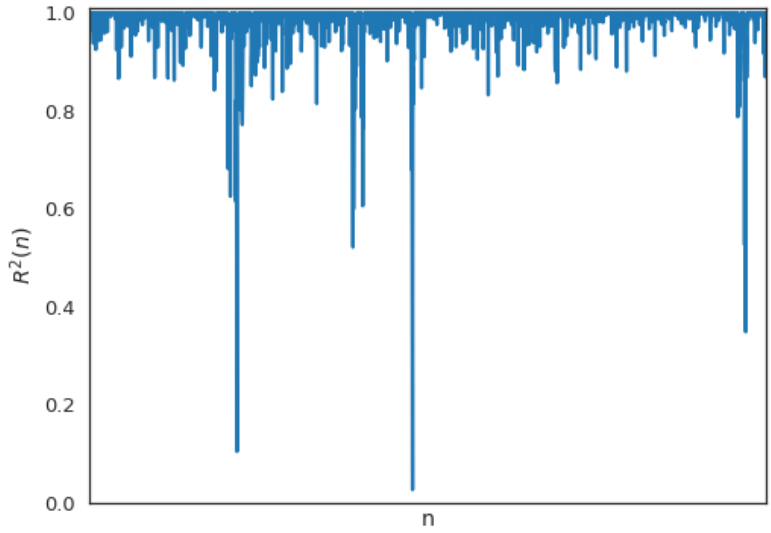

FIGURE 5.2: Consistency ratio $R^2(n)$ for Experiment 2.

was more varied than in Experiment 2; dramatic drops in model consistency were observed in many trials. The minimum median consistency of any single trial was 0.8798, and 47% of trials had consistency less than 0.999.

Discussion

The findings of Hancock et al. (2003) were replicated in the driving simulator environment, and MLDPE was able to describe this effect of distraction in terms of parameter dynamics. Specifically, a weaker attractor strength for braking was observed under distraction conditions. Here, a within-subjects manipulation was used, decoupling the ϵ values from the β coefficients. This demonstrates the applicability of MLDPE to a wider variety of experimental designs.

Future work should consider other effects observed in Hancock et al. (2003) and the wider driving literature, including effects of age, gender, and driving conditions. This initial validation of MLDPE suggests that these effects can be described not only in terms of summary measures such as response time and stopping time, but also in terms of differences in the underlying dynamics. Further investigation along these lines will lead to a more precise understanding of driving safety; for example, knowledge of the dynamics will allow for interventions to be tested in simulation studies before they are tested with human drivers.

Chapter 6

Conclusions

Multi-level dynamical parameter estimation (MLDPE) allows for parameter-selection problems to be solved that were previously impossible. However, in Experiment 1, the limitations of the method were met, specifically with respect to non-smooth functions. In Experiments 2 and 3, we showed that MLDPE can allow parameters to vary systematically according to the experimental condition. In this way, parameter values can become dependent variables in experimental designs, allowing researchers to test hypotheses formulated in terms of the impact that the experimental manipulation has on the dynamics of a system.

MLDPE, therefore, may offer a new role for dynamical models to play in a research program. They need not merely be descriptive, or proofs of concept. Rather, dynamical models can be used as test beds for manipulating and measuring parameter dynamics (Saltzman & Munhall, 1992). Parameters should not be expected to always remain constant, but we rarely observe systems long enough to treat parameters as a function of time. Instead, we can treat them as varying over realizations, perhaps by sampling unit or by experimental condition. In the experiments described here, the only sampling unit used was participant, but in general

any sampling unit, even nested units, can be used, as in repeated-measures designed and hierarchical regression. Additionally, Experiments 2 and 3 used only two-condition designs to test systematic variation in model parameters, but more complex design matrices can be used.

The success of MLDPE in larger problems with more complicated designs will depend highly on the accuracy of the model. It should not be controversial to state that the models used in behavioral dynamics are far less accurate than those in fields such as engineering. As much as we may hope that a low-dimensional predictable behavior emerges from the interaction between agent and environment (Kelso, 1995; Warren, 2006), this is only a generalization and necessary simplification. In fact, observed behavior even in a constrained experimental setting, is high-dimensional, and there will always be perturbations and other unexplained deviations from model predictions. It will never be easy to determine whether a model is correctly formulated, as it is never completely formulated, nor should it be. Therefore, a better test of MLDPE may arise from a field where dynamical predictions are typically more accurate than they are at the level of behavioral dynamics.

In the philosophy of science, the relationship between models, theories, and data has been complicated (Frigg & Hartmann, 2017; Morgan & Morrison, 1999). In behavioral dynamics, we use models to illustrate our theories and to demonstrate the feasibility of dynamical explanations without cognitive representation (Warren, 2006). Relating models to data is seen as important, but perhaps only secondary to the qualitative behavior of the model: the topology of attractors, repellers, and bifurcations that describe the system's behavior. However, data has a role to play in modeling besides simply validating that a model is correct (or correct enough). In addition, we can use data to drive changes in our models, and therefore to answer empirical questions about our systems of interest. MLDPE allows us to do measure these changes in terms of parameter dynamics, allowing the model to become

a bridge between data and theory.

Limitations

Unfortunately, MLDPE does not meet all the requirements for the ideal parameter-selection method that were set out in the Introduction.

It is still computationally expensive; whereas the black-box method is limited by the number of parameters, MLDPE is limited by the number of observed timesteps (and therefore also by the number of trials). As a result, the complete dataset for each experiment could not be analyzed, even with aggressive downsampling.

For this project, the open-source optimizer Ipopt (Wächter & Biegler, 2006) was used, as it resulted in the best performance compared to the other solvers that were tried, sequential least squares as implemented in NLopt (Johnson, 2014) and SciPy (Jones et al., 2001–). Nevertheless, high-memory Google Compute Engine instances were required to run these analyses. Commercial optimizer packages were not explored; it is likely that an option such as SNOPT (Gill, Murray, & Saunders, 2005) would result in increased performance and greater efficiency, allowing MLDPE to be run on researcher's personal computers rather than in the cloud.

MLDPE also does not get rid of hyperparameters, optimization settings that must be tweaked for best performances. Thus, the researcher degrees of freedom problem remains (Simmons et al., 2011). Nevertheless, there are fewer choices required than with the black-box method. Primarily, the researcher must choose values for c_p in order to determine how to weigh errors in the hypothesized parameter relationships against errors in the fit to data. It is difficult to imagine how this choice can be obviated. A benefit of MLDPE, at

the least, is that this is a domain-general choice rather than a domain-specific one. That is, the parameter selection process need not be developed anew for each system as with the black-box method.

Finally, the inability to converge on a solution in Experiment 1 points to a fundamental limitation of local optimization routines, that they are incompatible with non-smooth functions. Global, heuristic search may be the only option available for such problems.

Future work

As presented here, MLDPE is lacking several respects. Most notably, there is no method for comparing one set of parameters to another. For example, if a parameter is allowed to vary by participant, this will undoubtedly increase the fit because the problem's degrees of freedoms are increased. What is required is a method of asking whether the improved fit is "worth" the additional degrees of freedom. Perhaps these considerations would be weighed against each other heuristically, similar to the Akaike (1998) information criterion. However, lacking likelihood functions, something new must be developed specifically for MLDPE, perhaps relating to Abarbanel et al.'s (2009) proposed model consistency, Equation 1.13. However, discrepancies were observed between consistency and subjective model fit, and so a closer look at Equation 1.13 is warranted before using it for other purposes.

Similarly, we would like to be able to perform significance tests on fixed effects in parameter relationships. This would require a similar procedure as in the previous paragraph. Similar to in analyses of variance (ANOVA), we might be able to compare the results with the fixed effect to those without the fixed effect. That this would require running the MLDPE optimization twice is unfortunate, but this may be unavoidable. It would be required not

only to develop a comparison metric, but also to construct a confidence interval in order to determine significance, or something akin to it. Bootstrapping would be a viable option here, but it would take a very long time to run for any serious problem. Perhaps efficiency gains from using commercial solvers would make bootstrapping a reasonable option for the construction of confidence intervals around estimated parameter values.

Finally, it remains for MLDPE to be released as an open-source package, so that it may be easily used by other scientists. Such a release is forthcoming, but it requires a general interface, usage tests, and syntactical documentation in addition to the motivational and mathematical description contained in this dissertation. These additional elements were out of scope for this project, but once they are ready, the software behind this dissertation will be made available under an open-source license.

Keeping in mind the limitations discussed above, MLDPE has applications to a number of research lines that utilize dynamical models to understand perception-action. In general, any case where the change of interest can be expressed as parameter dynamics is well-suited to analysis using MLDPE. The development of motor behavior, skill acquisition and motor learning, injury recovery, habit formation, among other phenomena, can be considered as "second-order" dynamics—dynamics of dynamics. From this perspective, the ability to use existing dynamical models to test for systematic change in the behavior of a system would be valuable. Any theory that makes predictions regarding how the behavioral dynamics of goal-directed behavior change over time (e.g., Davids, Araújo, Vilar, Renshaw, & Pinder, 2013; Jacobs & Michaels, 2007; Mitra, Amazeen, & Turvey, 1998; Müller & Sternad, 2004; Scholz & Schöner, 1999) could be tested using the method described here, given a suitable dynamical model. With the necessary refinements of the method, in particular improved computational efficiency and an alternative to hypothesis testing, MLDPE would be a powerful tool for these and other fields of study. This would more completely manifest van Gelder's (1998)

dynamical hypothesis, demonstrating not only the utility of dynamical thinking, but also the direct relevance of dynamical modeling to experimental research.

References

Abarbanel, H. D., Creveling, D. R., Farsian, R., & Kostuk, M. (2009). Dynamical state and parameter estimation. *SIAM Journal on Applied Dynamical Systems*, *8*(4), 1341–1381.

Akaike, H. (1998). Information theory and an extension of the maximum likelihood principle. In *Selected papers of hirotugu akaike* (pp. 199–213).

Balasubramaniam, R., Riley, M. A., & Turvey, M. T. (2000). Specificity of postural sway to the demands of a precision task. *Gait & posture*, *11*(1), 12–24.

Batty, M., DeSyllas, J., & Duxbury, E. (2003). The discrete dynamics of small-scale spatial events: Agent-based models of mobility in carnivals and street parades. *International Journal of Geographical Information Science*, *17*(7), 673–697.

Biscani, F., Izzo, D., & Yam, C. H. (2010). A global optimization toolbox for massively parallel engineering optimisation. In *4th international conference on aerodynamics tools and techniques (ICATT 2010).*

Bonneaud, S., Rio, K., Chevaillier, P., & Warren, W. H. (2012). Accounting for patterns of collective behavior in crowd locomotor dynamics for realistic simulations. *Trans. Edutainment*, *7*, 1–11.

Bruggeman, H., Cohen, J. A., Harrison, H. S., & Warren, W. H. (2013). *Behavioral dynamics of moving obstacle avoidance.* (Unpublished manuscript)

Chapman, S. (1968). Catching a baseball. *American Journal of Physics*, *36*, 868.

Chardenon, A. B., & Warren, W. H. (2004). Intercepting moving targets on foot: Control of walking speed and direction. *Journal of Vision*, *4*(8), 805–805.

Cinelli, M. E., Patla, A. E., & Allard, F. (2008). Strategies used to walk through a moving aperture. *Gait & posture*, *27*(4), 595–602.

Cohen, J. A., Bruggeman, H., & Warren, W. H. (2005). Switching behavior in moving obstacle avoidance. *Journal of Vision*, *5*(8), 312–312.

Cohen, J. A., Bruggeman, H., & Warren, W. H. (2006). Combining moving targets and moving obstacles in a locomotion model. *Journal of Vision*, *6*(6), 135–135.

Dachner, G. C., & Warren, W. H. (2014). Behavioral dynamics of heading alignment in pedestrian following. *Transportation Research Procedia*, *2*, 69–76.

Davids, K., Araújo, D., Vilar, L., Renshaw, I., & Pinder, R. (2013). An ecological dynamics approach to skill acquisition: implications for development of talent in sport. *Talent Development and Excellence*, *5*(1), 21–34.

Dixon, J. A., Holden, J. G., Mirman, D., & Stephen, D. G. (2012). Multifractal dynamics in the emergence of cognitive structure. *Topics in Cognitive Science*, *4*(1), 51–62.

Fajen, B. R. (2007). Affordance-based control of visually guided action. *Ecological Psychology*, *19*(4), 383–410.

Fajen, B. R., Riley, M. A., & Turvey, M. T. (2009). Information, affordances, and the control of action in sport. *International Journal of Sport Psychology*, *40*(1), 79–107.

Fajen, B. R., & Warren, W. H. (2003). Behavioral dynamics of steering, obstable avoidance, and route selection. *Journal of Experimental Psychology: Human Perception and Performance*, *29*(2), 343–362.

Fajen, B. R., & Warren, W. H. (2004). Visual guidance of intercepting a moving target on foot. *Perception*, *33*, 689–716.

Fajen, B. R., & Warren, W. H. (2007). Behavioral dynamics of intercepting a moving target. *Experimental Brain Research*, *180*(2), 303–319.

Fink, P. W., Foo, P. S., & Warren, W. H. (2009). Catching fly balls in virtual reality: A critical test of the outfielder problem. *Journal of Vision*, *9*(13), 14.

Frank, T. D., Profeta, V. L. S., & Harrison, H. S. (2015). Interplay between order-parameter and system parameter dynamics: considerations on perceptual-cognitive-behavioral mode-mode transitions exhibiting positive and negative hysteresis and on response times. *Journal of biological physics*, *41*(3), 257–292.

Frigg, R., & Hartmann, S. (2017). Models in science. In E. N. Zalta (Ed.), *The stanford encyclopedia of philosophy* (Spring 2017 ed.). Metaphysics Research Lab, Stanford University. https://plato.stanford.edu/archives/spr2017/entries/models-science/.

Gérin-Lajoie, M., Richards, C. L., Fung, J., & McFadyen, B. J. (2008). Characteristics of personal space during obstacle circumvention in physical and virtual environments. *Gait & posture*, *27*(2), 239–247.

Gérin-Lajoie, M., Richards, C. L., & McFadyen, B. J. (2005). The negotiation of stationary and moving obstructions during walking: Anticipatory locomotor adaptations and preservation of personal space. *Motor control*, *9*(3), 242–269.

Gibson, J. J. (1958). Visually controlled locomotion and visual orientation in animals. *British journal of psychology*, *49*(3), 182–194.

Gibson, J. J. (1979/1986). *The ecological approach to visual perception*. Hillsdale, NJ: Lawrence Erlbaum.

Gill, P. E., Murray, W., & Saunders, M. A. (2005). SNOPT: An SQP algorithm for large-scale constrained optimization. *SIAM review*, *47*(1), 99–131.

Hackney, A. L., Vallis, L. A., & Cinelli, M. E. (2013). Action strategies of individuals

during aperture crossing in nonconfined space. *The Quarterly Journal of Experimental Psychology*, *66*(6), 1104–1112.

Haken, H., Kelso, J. A. S., & Bunz, H. (1985). A theoretical model of phase transitions in human hand movements. *Biological cybernetics*, *51*(5), 347–356.

Hancock, P. A., Lesch, M., & Simmons, L. (2003). The distraction effects of phone use during a crucial driving maneuver. *Accident Analysis & Prevention*, *35*(4), 501–514.

Harrison, H. S., Kelty-Stephen, D. G., Vaz, D. V., & Michaels, C. F. (2014). Multiplicative-cascade dynamics in pole balancing. *Physical Review E*, *89*(6), 060903.

Harrison, H. S., Turvey, M. T., & Frank, T. D. (2016). Affordance-based perception-action dynamics: A model of visually guided braking. *Psychological Review*, *123*(3), 305.

Helbing, D., & Molnar, P. (1995). Social force model for pedestrian dynamics. *Physical Review E*, *51*(5), 4282.

Hindmarsh, A. C. (1983). ODEPACK, a systematized collection of ODE solvers. In R. S. Stepleman (Ed.), *IMACS transactions on scientific computation* (Vol. 1, pp. 55–64). North-Holland.

Hunter, J. D. (2007). Matplotlib: A 2D graphics environment. *Computing In Science & Engineering*, *9*(3), 90–95.

Jacobs, D. M., & Michaels, C. F. (2007). Direct learning. *Ecological psychology*, *19*(4), 321–349.

Johnson, S. G. (2014). *The NLopt nonlinear-optimization package.* Retrieved from http://ab-initio.mit.edu/wiki/index.php/NLopt

Jones, E., Oliphant, O., Peterson, P., et al. (2001–). *SciPy: Open source scientific tools for Python.* Retrieved from http://www.scipy.org/

Kelso, J. A. S. (1995). *Dynamic patterns: The self-organization of brain and behavior.* Cambridge, MA: MIT Press.

Kelty-Stephen, D. G., Palatinus, K., Saltzman, E., & Dixon, J. A. (2013). A tutorial on multifractality, cascades, and interactivity for empirical time series in ecological science. *Ecological Psychology*, *25*(1), 1–62.

Khatib, O. (1986). Real-time obstacle avoidance for manipulators and mobile robots. *The international journal of robotics research*, *5*(1), 90–98.

Klügl, F., & Rindsfüser, G. (2007). Large-scale agent-based pedestrian simulation. In *German conference on multiagent system technologies* (pp. 145–156).

Kugler, P. N., & Turvey, M. T. (1987). *Information, natural law, and the self-assembly of rhythmic movement*. Hillsdale, NJ: Lawrence Erlbaum.

Lee, D. N. (1976). A theory of visual control of braking based on information about time-to-collision. *Perception*, *5*(4), 437–459.

Lopresti-Goodman, S. M., Turvey, M. T., & Frank, T. D. (2013). Negative hysteresis in the behavioral dynamics of the affordance "graspable". *Attention, Perception, & Psychophysics*, *75*(5), 1075–1091.

Luenberger, D. G. (1964). Observing the state of a linear system. *IEEE transactions on military electronics*, *8*(2), 74–80.

Luenberger, D. G. (1966). Observers for multivariable systems. *IEEE Transactions on Automatic Control*, *11*(2), 190–197.

Luenberger, D. G. (1971). An introduction to observers. *IEEE Transactions on automatic control*, *16*(6), 596–602.

McLeod, P., Reed, N., & Dienes, Z. (2006). The generalized optic acceleration cancellation theory of catching. *Journal of Experimental Psychology: Human Perception and Performance*, *32*(1), 139–148.

Michaels, C. F., & Carello, C. (1981). *Direct perception*. Englewood Cliffs, NJ: Prentice-Hall.

Michaels, C. F., & Oudejans, R. R. D. (1992). The optics and actions of catching fly balls:

Zeroing out optical acceleration. *Ecological Psychology*, *4*(4), 199–222.

Michaels, C. F., & Zaal, F. T. (2002). Catching fly balls. In S. Bennett, K. Davids, G. J. Savelsbergh, & J. van der Kamp (Eds.), *Interceptive actions in sport: Information and movement* (pp. 172–83). London: Routledge.

Mitra, S., Amazeen, P. G., & Turvey, M. T. (1998). Intermediate motor learning as decreasing active (dynamical) degrees of freedom. *Human Movement Science*, *17*(1), 17–65.

Morgan, M. S., & Morrison, M. (1999). *Models as mediators: Perspectives on natural and social science*. Cambridge, UK: Cambridge Unversity Press.

Müller, H., & Sternad, D. (2004). Decomposition of variability in the execution of goal-oriented tasks: three components of skill improvement. *Journal of Experimental Psychology: Human Perception and Performance*, *30*(1), 212.

Pires, C., Vautard, R., & Talagrand, O. (1996). On extending the limits of variational assimilation in nonlinear chaotic systems. *Tellus A*, *48*(1), 96–121.

Quinn, J. C., Bryant, P. H., Creveling, D. R., Klein, S. R., & Abarbanel, H. D. (2009). Parameter and state estimation of experimental chaotic systems using synchronization. *Physical Review E*, *80*(1), 016201.

Richardson, M. J., Harrison, S. J., Kallen, R. W., Walton, A., Eiler, B. A., Saltzman, E., & Schmidt, R. C. (2015). Self-organized complementary joint action: Behavioral dynamics of an interpersonal collision-avoidance task. *Journal of Experimental Psychology: Human Perception and Performance*, *41*(3), 665.

Riley, M. A., Balasubramaniam, R., & Turvey, M. T. (1999). Recurrence quantification analysis of postural fluctuations. *Gait & posture*, *9*(1), 65–78.

Roduit, P. (2009). *Trajectory analysis using point distribution models* (Unpublished doctoral dissertation). École polytechnique fédérale de Lausanne.

Saltzman, E. L., & Munhall, K. G. (1992). Skill acquisition and development: The roles of state-, parameter-, and graph-dynamics. *Journal of Motor Behavior*, *24*(1), 49–57.

Schmidt, R. C., Carello, C., & Turvey, M. T. (1990). Phase transitions and critical fluctuations in the visual coordination of rhythmic movements between people. *Journal of Experimental Psychology: Human Perception and Performance*, *16*(2), 227–247.

Scholz, J. P., & Schöner, G. (1999). The uncontrolled manifold concept: Identifying control variables for a functional task. *Experimental brain research*, *126*(3), 289–306.

Shaw, R., & Kinsella-Shaw, J. (1988). Ecological mechanics: A physical geometry for intentional constraints. *Human movement science*, *7*(2), 155–200.

Simmons, J. P., Nelson, L. D., & Simonsohn, U. (2011). False-positive psychology: Undisclosed flexibility in data collection and analysis allows presenting anything as significant. *Psychological Science*, *22*(11), 1359–1366.

Stephen, D. G., & Dixon, J. A. (2011). Strong anticipation: Multifractal cascade dynamics modulate scaling in synchronization behaviors. *Chaos, Solitons & Fractals*, *44*(1), 160–168.

Takens, F. (1981). Detecting strange attractors in turbulence. *Lecture notes in mathematics*, *898*(1), 366–381.

Thelen, E., & Smith, L. B. (1994). *A dynamic system approach to the development of cognition and action*. Cambridge, MA: MIT Press.

Turvey, M. T., & Carello, C. (1986). The ecological approach to perceiving-acting: A pictorial essay. *Acta Psychologica*, *63*(2), 133–155.

van der Walt, S., Colbert, S. C., & Varoquaux, G. (2011). The NumPy array: a structure for efficient numerical computation. *Computing in Science & Engineering*, *13*(2), 22–30.

van Gelder, T. (1998). The dynamical hypothesis in cognitive science. *Behavioral and Brain Sciences*, *21*(5), 615–628.

Voss, H. U., Timmer, J., & Kurths, J. (2004). Nonlinear dynamical system identification from uncertain and indirect measurements. *International Journal of Bifurcation and Chaos*, *14*(06), 1905–1933.

Warren, W. H. (1988). Action modes and laws of control for the visual guidance of action. In O. G. Meijer & K. Roth (Eds.), *Complex movement behaviour: The motor-action controversy* (Vol. 50, pp. 339–380). Amsterdam: North-Holland.

Warren, W. H. (2006). The dynamics of perception and action. *Psychological Review*, *113*(2), 358–389.

Warren, W. H., & Fajen, B. R. (2004). Behavioral dynamics of human locomotion. *Ecological Psychology*, *16*(1), 61-66.

Warren, W. H., & Fajen, B. R. (2008). Behavioral dynamics of visually guided locomotion. *Coordination: Neural, Behavioral and Social Dynamics*, 45–75.

Warren, W. H., Kay, B. A., Zosh, W. D., Duchon, A. P., & Sahuc, S. (2001). Optic flow is used to control human walking. *Nature Neuroscience*, *4*(2), 213-216.

Waskom, M., Botvinnik, O., O'Kane, D., et al. (2017). *mwaskom/seaborn: v0.8.0 (july 2017).* Retrieved from https://doi.org/10.5281/zenodo.824567 doi: 10.5281/zenodo.824567

Wächter, T., & Biegler, L. T. (2006). On the implementation of a primal-dual interior point filter line search algorithm for large-scale nonlinear programming. *Mathematical Programming*, *106*(1), 25–57.

Yersin, B., Maïm, J., Pettré, J., & Thalmann, D. (2009). Crowd patches: populating large-scale virtual environments for real-time applications. In *Proceedings of the 2009 symposium on interactive 3d graphics and games* (pp. 207–214).

Čertík, O., Peterson, D. L., et al. (2015–). *SymEngine: A fast symbolic manipulation library, written in C++.* Retrieved from https://github.org/symengine/symengine